

Phosphorylation of Yeast Pah1 Phosphatidate Phosphatase by Casein Kinase II Regulates Its Function in Lipid Metabolism*

Received for publication, March 9, 2016, and in revised form, March 31, 2016. Published, JBC Papers in Press, April 4, 2016, DOI 10.1074/jbc.M116.726588

Lu-Sheng Hsieh, Wen-Min Su, Gil-Soo Han, and George M. Carman¹

From the Department of Food Science and the Rutgers Center for Lipid Research, New Jersey Institute for Food, Nutrition, and Health, Rutgers University, New Brunswick, New Jersey 08901

Pah1 phosphatidate phosphatase in *Saccharomyces cerevisiae* catalyzes the penultimate step in the synthesis of triacylglycerol (*i.e.* the production of diacylglycerol by dephosphorylation of phosphatidate). The enzyme playing a major role in lipid metabolism is subject to phosphorylation (*e.g.* by Pho85-Pho80, Cdc28-cyclin B, and protein kinases A and C) and dephosphorylation (*e.g.* by Nem1-Spo7) that regulate its cellular location, catalytic activity, and stability/degradation. In this work, we show that Pah1 is a substrate for casein kinase II (CKII); its phosphorylation was time- and dose-dependent and was dependent on the concentrations of Pah1 ($K_m = 0.23 \mu\text{M}$) and ATP ($K_m = 5.5 \mu\text{M}$). By mass spectrometry, truncation analysis, site-directed mutagenesis, phosphopeptide mapping, and phosphoamino acid analysis, we identified that >90% of its phosphorylation occurs on Thr-170, Ser-250, Ser-313, Ser-705, Ser-814, and Ser-818. The CKII-phosphorylated Pah1 was a substrate for the Nem1-Spo7 protein phosphatase and was degraded by the 20S proteasome. The prephosphorylation of Pah1 by protein kinase A or protein kinase C reduced its subsequent phosphorylation by CKII. The prephosphorylation of Pah1 by CKII reduced its subsequent phosphorylation by protein kinase A but not by protein kinase C. The expression of Pah1 with combined mutations of S705D and 7A, which mimic its phosphorylation by CKII and lack of phosphorylation by Pho85-Pho80, caused an increase in triacylglycerol content and lipid droplet number in cells expressing the Nem1-Spo7 phosphatase complex.

The PAP² enzyme (EC 3.1.3.4) catalyzes the Mg²⁺-dependent dephosphorylation of PA to produce DAG (1) (Fig. 1A). Because PAP controls the cellular levels of its substrate PA, which is used for the synthesis of essential membrane phospholipids (*e.g.* phosphatidylinositol) via CDP-DAG, and its product DAG, which is used for the synthesis of TAG and the membrane phospholipids phosphatidylcholine and phosphatidylethanolamine, the enzyme is widely recognized for its key reg-

ulatory role in lipid metabolism (2–8). Although it was identified in 1957 (1), it was not purified to near homogeneity until 1989 (9), and it took another 17 years before the *PAH1* gene encoding the enzyme was identified in yeast³ (10). This discovery led to the revelation that mammalian lipin proteins, whose molecular function had not been known (11), were in fact PAP enzymes (10, 12). The analyses of yeast and mammalian cells that lack PAP have shown that this enzyme is a major regulator of lipid homeostasis and cell physiology (2, 3, 6, 8, 13, 14). For example, in yeast, PAP activity regulates phospholipid synthesis and nuclear/ER membrane growth (10, 15–18), the synthesis of TAG, the formation of lipid droplets (10, 17–19), vacuole homeostasis (20), and cell wall integrity (21, 22).

Insight into the expression, mode of action, and biochemical regulation of PAP has been gained through studies on the yeast enzyme (Fig. 1A) (2, 3, 13, 23, 24). The expression of *PAH1* is regulated at the transcriptional level by growth phase and nutrient status (18, 25). The transcription of *PAH1* is induced throughout growth, and its induction in the stationary phase is enhanced by inositol supplementation (18). This transcriptional regulation is mediated through the Ino2/Ino4/Opi1 regulatory circuit and by the transcription factors Gis1 and Rph1 (18). The *PAH1* expression is also induced by zinc deficiency in the exponential phase through the Zap1-mediated transcriptional activation, resulting in an increase in synthesis of phosphatidylcholine via the CDP-choline branch of the Kennedy pathway (25). In contrast, the induction of *PAH1* expression in zinc-replete stationary phase cells is responsible for increased synthesis and the accumulation of TAG that occurs at the expense of phospholipid synthesis (18). In response to growth phase and nutrient status, transcription factors that induce the *PAH1* expression have negative regulatory effects on phospholipid synthesis genes (26, 27), and the opposing regulations collectively contribute to the balanced synthesis of membrane phospholipids and TAG.

The activity of Pah1 is governed by a conserved DXDX(T/V) catalytic motif within its haloacid dehalogenase-like domain and by a conserved glycine residue within its NLIP domain (10, 11, 16, 28, 29) (Fig. 1B). The enzyme is stimulated by negatively charged phospholipids (*e.g.* CDP-DAG and phosphatidylinositol) that increase its affinity for PA (30), but it is inhibited by positively charged sphingoid bases (*e.g.* sphinganine and phyto-

* This work was supported, in whole or in part, by National Institutes of Health Grant GM050679 from the United States Public Health Service. The authors declare that they have no conflicts of interest with the contents of this article.

¹ To whom correspondence should be addressed: Dept. of Food Science, Rutgers University, 65 Dudley Rd., New Brunswick, NJ 08901. Tel.: 848-932-5407; E-mail: carman@aesop.rutgers.edu.

² The abbreviations used are: PAP, phosphatidate phosphatase; PA, phosphatidate; TAG, triacylglycerol; DAG, diacylglycerol; CKII, casein kinase II; ER, endoplasmic reticulum; SC, synthetic complete.

³ In this paper, the term yeast is used interchangeably with *Saccharomyces cerevisiae*.

sphingosine) that decrease its affinity for PA (31). It is also inhibited by ATP and CTP through a complex mechanism that affects both the V_{\max} and the K_m for PA and through a chelating effect on the cofactor Mg^{2+} (32). As a peripheral membrane protein (10), Pah1 associates with the nuclear/ER membrane through its dephosphorylation, which is catalyzed by an integral membrane protein phosphatase consisting of Nem1 (catalytic subunit) and Spo7 (regulatory subunit) (15, 33–41) (Fig. 1A). Its interaction with the Nem1-Spo7 complex occurs through the C-terminal acidic tail (39), whereas its membrane association occurs through the N-terminal amphipathic helix (36) (Fig. 1B). The dephosphorylation of Pah1 by Nem1-Spo7 also regulates its PAP activity and degradation by the 20S proteasome (15, 33, 35, 37, 38, 40, 42–45).

Pah1 is a phosphoprotein in the cytosol, and its phosphorylation is carried out by multiple protein kinases. Pah1 has been shown by phosphoproteomic studies to be phosphorylated on more than 30 serine/threonine sites (33, 46–51) and is a target for various protein kinases *in vitro* (40, 49). Our laboratory has taken a systematic approach to identify protein kinases that phosphorylate Pah1, to determine its phosphorylation sites, and to reveal the physiological relevance of its phosphorylation. We have shown that Pah1 is a *bona fide* substrate for Pho85-Pho80 (37), Cdc28-cyclin B (35), protein kinase A (38), and protein kinase C (42) by determining its phosphorylation sites (Fig. 1B). Some of the phosphorylation sites regulate the localization of Pah1, its PAP activity, or susceptibility to the 20S proteasomal degradation (35, 37, 38, 42). Moreover, the phosphorylation of Pah1 on some sites influences its phosphorylation on other sites by the same protein kinase or different protein kinases, indicating that it is subject to hierarchical phosphorylation (38, 42).

In a previous study (40), we have shown that Pah1 is phosphorylated by CKII, a highly conserved serine/threonine protein kinase that is essential for cell viability in yeast (52–55). The protein kinase is composed of two catalytic (*i.e.* Cka1 and Cka2) and two regulatory (*i.e.* Ckb1 and Ckb2) subunits (55–59). CKII generally phosphorylates proteins with the motif (S/T)XX(E/D) but will also phosphorylate proteins with (S/T)X(E/D) or (S/T)(E/D) (56–58, 60). In this work, we have characterized the CKII-mediated phosphorylation of Pah1 and identified its phosphorylation sites (Fig. 1B). We also examined the CKII phosphorylation of Pah1 in relation to its phosphorylation by other protein kinases, the dephosphorylation of the CKII-phosphorylated Pah1 by the Nem1-Spo7 phosphatase, and the physiological consequences of cells expressing Pah1 with its CKII site mutations. The mutational analysis of Pah1 indicated that it regulates the synthesis of TAG and the number of lipid droplets through its cross-talk phosphorylation by the protein kinases CKII and Pho85-Pho80 as well as through its dephosphorylation by Nem1-Spo7 phosphatase.

Experimental Procedures

Reagents—Avanti Polar Lipids was the source of all lipids. Bradford (61) protein reagent, DNA size ladders, molecular mass protein standards, and reagents for electrophoresis and immunoblotting were obtained from Bio-Rad. Clontech was the supplier of carrier DNA for yeast transformation. Difco was

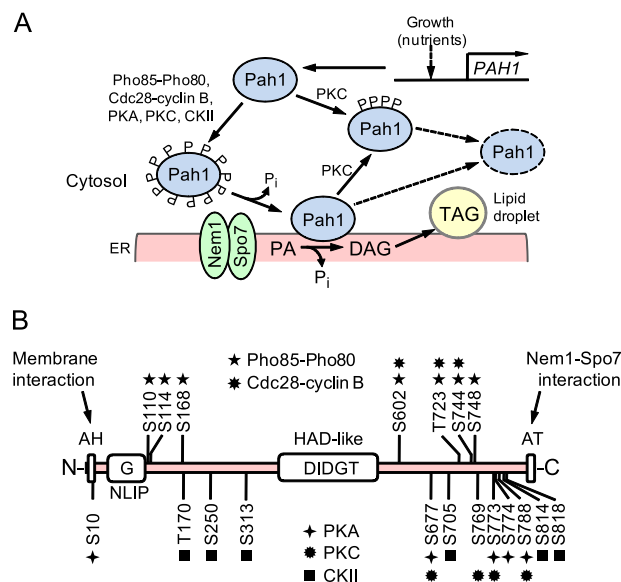


FIGURE 1. Model for the genetic and biochemical regulations of Pah1 PAP. A, the expression of *PAH1* is regulated during growth by nutrient status as mediated by the Ino2/Ino4/Opi1 regulatory circuit and transcription factors Gis1, Rph1, and Zap1 (18, 25). Pah1 in the cytosol is phosphorylated by multiple protein kinases that include Pho85-Pho80 (37), Cdc28-cyclin B (35), PKA (38), PKC (42), and CKII (this study). The phosphorylated enzyme (Pah1 decorated with the letter P) translocates to the ER membrane through its dephosphorylation by the Nem1-Spo7 phosphatase complex. Dephosphorylated Pah1 that is associated with the ER catalyzes the conversion of PA to DAG, which is then acylated to form TAG that is then stored in lipid droplets. Dephosphorylated Pah1 or PKC-phosphorylated Pah1 that is not phosphorylated at Pho85-Pho80/Cdc28-cyclin B sites is degraded by the 20S proteasome (45) (indicated by the dashed line arrow and ellipse). B, diagram of Pah1 domain structure showing the positions of the amphipathic helix (AH) required for ER membrane interaction (36); the NLIP and HAD-like domains containing the conserved glycine (G) and DIDGT catalytic sequence, respectively, that are required for PAP activity (16); the acidic tail (AT) required for interaction with Nem1-Spo7 (39); and the serine (S) and threonine (T) residues that are phosphorylated by Pho85-Pho80 (37), Cdc28-cyclin B (35), PKA (38), PKC (42), and CKII (this study).

the supplier of growth media. EMD Millipore was the source of cellulose and silica gel 60 TLC plates. GE Healthcare was the source of IgG-Sepharose, Q-Sepharose, PVDF membrane, and the enhanced chemifluorescence Western blotting detection kit. The yeast deletion consortium strains were from Invitrogen. National Diagnostics and PerkinElmer Life Sciences were the sources of scintillation counting supplies and radiochemicals, respectively. New England Biolabs was the source of enzyme reagents for DNA manipulations, human casein kinase II, and cyclin-dependent kinase-cyclin B. Promega was the source of bovine heart protein kinase A catalytic subunit and rat brain conventional protein kinase C. Qiagen was the source of nickel-nitilotriacetic acid-agarose resin and the DNA gel extraction and plasmid DNA purification kits. Sigma-Aldrich was the source of ATP, PCR primers, L-1-tosylamido-2-phenylethyl chloromethyl ketone-trypsin, protease and phosphatase inhibitors, phosphoamino acid standards, Triton X-100, Ponceau S stain, bovine serum albumin, and rabbit anti-Protein A antibodies (product P3775, lot 053M4806V). Stratagene was the supplier of the QuikChange site-directed mutagenesis kit. Thermo Scientific was the source of mouse anti-phosphoglycerate kinase antibodies (product 459250, lot 459250/E1161), alkaline phosphatase-conjugated goat anti-rabbit IgG antibodies (product 31340, lot NJ178812), alkaline phosphatase

Phosphorylation of Pah1 Phosphatidate Phosphatase by CKII

TABLE 1
Strains used in this work

Strain	Relevant characteristics	Source/Reference
<i>E. coli</i>		
DH5 α	F ⁻ ϕ 80dlacZ Δ M15 Δ (<i>lacZYA-argF</i>)U169 <i>deoR recA1 endA1 hsdR17</i> (<i>r_k⁻ m_k⁺</i>) <i>phoA supE44 λ thi-1 gyrA96 relA1</i>	Ref. 64
BL21(DE3)pLysS	F ⁻ <i>ompT hsdS_B</i> (<i>r_B⁻ m_B⁻</i>) <i>gal dcm</i> (DE3) pLysS	Novagen
<i>S. cerevisiae</i>		
BY4741-CKA2-TAP	TAP-tagged Cka2 expressed in strain BY4741	Thermo Scientific
BY4741- <i>cka1</i> Δ	<i>cka1</i> Δ :: <i>kanMX4</i> derivative of BY4741	Deletion consortium
BY4741- <i>cka2</i> Δ	<i>cka2</i> Δ :: <i>kanMX4</i> derivative of BY4741	Deletion consortium
BY4741- <i>ckb1</i> Δ	<i>ckb1</i> Δ :: <i>kanMX4</i> derivative of BY4741	Deletion consortium
BY4741- <i>ckb2</i> Δ	<i>ckb2</i> Δ :: <i>kanMX4</i> derivative of BY4741	Deletion consortium
RS453	MATa <i>ade2-1 his3-11,15 leu2-3,112 trp1-1 ura3-52</i>	Ref. 106
SS1026	<i>pah1</i> Δ :: <i>TRP1</i> derivative of RS453	Ref. 15
SS1132	<i>pah1</i> Δ :: <i>TRP1 nem1</i> Δ :: <i>HIS3</i> derivative of RS453	Ref. 35
W303-1A	MATa <i>ade2-1 can1-100 his3-11,15 leu2-3,112 trp1-1 ura3-1</i>	Ref. 107
GHY66	<i>pah1</i> Δ :: <i>URA3 app1</i> Δ :: <i>natMX4 dpp1</i> Δ :: <i>TRP1/Kan'</i> <i>lpp1</i> Δ :: <i>His3/Kan'</i> derivative of W303-1A	Ref. 90

tase-conjugated goat anti-mouse IgG antibodies (product 31322, lot PB1815636), His₆-tagged tobacco etch virus protease, BODIPY 493/503, and *Saccharomyces cerevisiae* strains that express TAP-tagged fusion proteins. All other chemicals were reagent grade.

Strains and Growth Conditions—The strains used in this study are listed in Table 1. *Escherichia coli* strains DH5 α and BL21(DE3)pLysS were used for the propagation of plasmids and for the expression of His₆-tagged proteins, respectively. The bacterial cells were grown at 37 °C in LB medium (1% tryptone, 0.5% yeast extract, 1% NaCl, pH 7.0). The growth medium was supplemented with ampicillin (100 μ g/ml) and chloramphenicol (34 μ g/ml) to select for cells carrying plasmids for the expression of proteins (62). The expression of proteins in *E. coli* cells bearing derivatives of plasmid pET-15b was induced with 1 mM isopropyl β -D-1-thiogalactopyranoside. *S. cerevisiae* cells expressing TAP-tagged proteins were grown at 30 °C in YEPD medium (1% yeast extract, 2% peptone, and 2% glucose) (63). *S. cerevisiae* mutants *cka1* Δ , *cka2* Δ , *ckb1* Δ , and *ckb2* Δ were used to assess the effect of CKII-mediated phosphorylation on the abundance of Pah1, whereas the mutants *pah1* Δ and *pah1* Δ *nem1* Δ were used to assess the physiological impact of phosphorylation-deficient/mimicking Pah1. The *pah1* Δ *app1* Δ *dpp1* Δ *lpp1* Δ mutant was used to assess the PAP activity of phosphorylation-deficient/mimicking Pah1 in response to temperature. The yeast were grown at 30 °C in standard synthetic complete (SC) medium containing 2% glucose (63). Appropriate amino acids were omitted from SC growth medium to select for cells carrying specific plasmids (63). Spectrophotometry (*A*₆₀₀) was used to estimate cell numbers in liquid cultures. Liquid growth medium was supplemented with agar (2% for yeast and 1.5% for *E. coli*) to prepare solid growth medium.

Plasmids and DNA Manipulations—Tables 2 and 3 contain a list of plasmids used in this study. Plasmid pGH313 directs the isopropyl β -D-1-thiogalactopyranoside-induced expression of His₆-tagged Pah1 in *E. coli* (10). Plasmid pGH315 directs low copy expression of Pah1 in *S. cerevisiae* (35). The isolation of genomic and plasmid DNA, PCR amplification, digestion, and ligation of DNA were performed by standard molecular techniques (64, 65). pGH313(1–700) was constructed by generating a nonsense mutation at the 701st codon of *PAH1* in pGH313. The derivatives of pGH313 and pGH315 that contain serine/

threonine-to-alanine/aspartate/glutamate mutations were constructed by QuikChange site-directed mutagenesis with appropriate templates and primers as described by Choi *et al.* (35). All mutations were confirmed by DNA sequencing. Plasmid transformations of *E. coli* (64) and *S. cerevisiae* (66) were performed as described previously.

Preparations of Enzymes and the 20S Proteasome—CKII (52, 59) was purified from *S. cerevisiae* cells expressing the TAP-tagged Cka2 by IgG-Sepharose affinity chromatography as described by O'Hara *et al.* (33). The purification of Protein A-tagged Cka2 was confirmed by immunoblot analysis using anti-Protein A antibodies. His₆-tagged tobacco etch virus protease was used to remove the Protein A tag from the purified fusion protein (45). *E. coli*-expressed His₆-tagged wild type and mutant forms of yeast Pah1 (10) and His₆-tagged Pho85-Pho80 protein kinase complex (67) were purified by affinity chromatography with nickel-nitrilotriacetic acid-agarose as described previously. The 20S proteasome was purified from yeast expressing TAP-tagged Pre1 by IgG-Sepharose affinity chromatography (68), followed by the removal of the Protein A tag with His₆-tagged tobacco etch virus protease (45). Protein content of the purified enzymes and 20S proteasome was estimated by the method of Bradford (61) using bovine serum albumin as a standard, and the purity of the protein preparations was assessed by SDS-PAGE (69).

Analysis of Phosphorylation Sites by Mass Spectrometry—The CKII-phosphorylated Pah1 was analyzed by mass spectrometry at the Rutgers Mass Spectrometry Center for Integrative Neuroscience Research. Phosphorylated Pah1 in SDS-polyacrylamide gel slices was subjected to trypsin digestion, and the resulting peptides were analyzed by matrix-assisted laser desorption ionization tandem time-of-flight mass spectrometry to identify phosphopeptide candidates (35). Based on the phosphopeptide ion inclusion list, quadrupole time-of-flight and Orbitrap liquid chromatography-mass spectrometry/mass spectrometry were performed to identify phosphorylation sites (35).

Analysis of Phosphoamino Acids and Phosphopeptides—Radioactively phosphorylated Pah1 was resolved by SDS-PAGE, transferred to the PVDF membrane, and hydrolyzed with 6 N HCl at 110 °C (for phosphoamino acid analysis) or proteolytically cleaved with L-1-tosylamido-2-phenylethyl chloromethyl ketone-trypsin (for phosphopeptide analysis)

TABLE 2

Plasmids used for Pah1 expression in *E. coli*

Plasmid	Relevant characteristics	Source/Reference
pET-15b	<i>E. coli</i> expression vector with N-terminal His ₆ tag fusion	Novagen
pGH313(1–862)	<i>PAH1</i> coding sequence inserted (full-length) into pET-15b	Ref. 10
pGH313(1–821)	<i>PAH1</i> (1–821 truncation) derivative of pGH313	Ref. 45
pGH313(1–700)	<i>PAH1</i> (1–700 truncation) derivative of pGH313	This study
pGH313(1–646)	<i>PAH1</i> (1–646 truncation) derivative of pGH313	Ref. 38
pGH313(235–752)	<i>PAH1</i> (235–752 truncation) derivative of pGH313	Ref. 38
pGH313(T170A)	<i>PAH1</i> (T170A) derivative of pGH313	This study
pGH313(T176A)	<i>PAH1</i> (T176A) derivative of pGH313	This study
pGH313(S250A)	<i>PAH1</i> (S250A) derivative of pGH313	This study
pGH313(S254A)	<i>PAH1</i> (S254A) derivative of pGH313	This study
pGH313(S311A)	<i>PAH1</i> (S311A) derivative of pGH313	This study
pGH313(S313A)	<i>PAH1</i> (S313A) derivative of pGH313	This study
pGH313(T315A)	<i>PAH1</i> (T315A) derivative of pGH313	This study
pGH313(T319A)	<i>PAH1</i> (T319A) derivative of pGH313	This study
pGH313(S320A)	<i>PAH1</i> (S320A) derivative of pGH313	This study
pGH313(S327A)	<i>PAH1</i> (S327A) derivative of pGH313	This study
pGH313(T364A)	<i>PAH1</i> (T364A) derivative of pGH313	This study
pGH313(S397A)	<i>PAH1</i> (S397A) derivative of pGH313	This study
pGH313(S475A)	<i>PAH1</i> (S475A) derivative of pGH313	This study
pGH313(S511A)	<i>PAH1</i> (S511A) derivative of pGH313	This study
pGH313(T517A)	<i>PAH1</i> (T517A) derivative of pGH313	This study
pGH313(T553A)	<i>PAH1</i> (T553A) derivative of pGH313	This study
pGH313(S613A)	<i>PAH1</i> (S613A) derivative of pGH313	This study
pGH313(S704A)	<i>PAH1</i> (S704A) derivative of pGH313	This study
pGH313(S705A)	<i>PAH1</i> (S705A) derivative of pGH313	This study
pGH313(S711A)	<i>PAH1</i> (S711A) derivative of pGH313	This study
pGH313(S814A)	<i>PAH1</i> (S814A) derivative of pGH313	This study
pGH313(T816A)	<i>PAH1</i> (T816A) derivative of pGH313	This study
pGH313(S818A)	<i>PAH1</i> (S818A) derivative of pGH313	This study
pGH313(S313A/S705A)	<i>PAH1</i> (S313A/S705A) derivative of pGH313	This study
pGH313(S250A/S705A/S814A)	<i>PAH1</i> (S250A/S705A/S814A) derivative of pGH313	This study
pGH313(4A) (CKII phosphorylation sites)	<i>PAH1</i> (T170A/S313A/S705A/S818A) derivative of pGH313	This study
pGH313(6A) (CKII phosphorylation sites)	<i>PAH1</i> (T170A/S250A/S313A/S705A/S814A/S818A) derivative of pGH313	This study
pGH313(5A) (PKA phosphorylation sites)	<i>PAH1</i> (S10A/S677A/S773A/S774A/S788A) derivative of pGH313	Ref. 38
pGH313(4A) (PKC phosphorylation sites)	<i>PAH1</i> (S677A/S769A/S773A/S788A) derivative of pGH313	Ref. 42
pGH313(7A) (pGH332) (Pho85-Pho80 phosphorylation sites)	<i>PAH1</i> (S110A/S114A/S168A/S602A/T723A/S744A/S748A) derivative of pGH313	Ref. 37

(70–72). The acid hydrolysates were mixed with standard phosphoamino acids and were separated by two-dimensional electrophoresis on cellulose TLC plates. The tryptic digests were separated on the cellulose plates first by electrophoresis and then by TLC (70–72). Radioactive phosphoamino acids and peptides were visualized by phosphorimaging analysis. Non-radioactive phosphoamino acid standards were visualized by ninhydrin staining.

Preparation of Cell Extracts and Subcellular Fractionation—All steps were performed at 4 °C. Cell extracts were prepared by disruption of cells with glass beads using a BioSpec Products Mini-BeadBeater-16 (73). The cell disruption buffer contained 50 mM Tris-HCl (pH 7.5), 0.3 M sucrose, 10 mM 2-mercaptoethanol, 0.5 mM phenylmethanesulfonyl fluoride, 1 mM benzamidine, 5 µg/ml aprotinin, 5 µg/ml leupeptin, 5 µg/ml pepstatin, and phosphatase inhibitor mixture I and II (10). The cytosolic (supernatant) and total membrane (pellet) fractions were separated by centrifugation at 100,000 × *g* for 1 h (73). The membrane pellets were suspended in the cell disruption buffer to the same volume of the cytosolic fraction. The method of Bradford (61) was used to estimate protein concentration with bovine serum albumin as a standard.

Immunoblotting—Proteins were separated by SDS-PAGE (69) using 8% slab gels. The samples for immunoblotting were normalized to total protein loading as determined by the Coomassie Blue-based assay of Bradford (61). Immunoblotting with PVDF membrane was performed as described previously (74–76). Protein transfer from SDS-polyacrylamide gels to PVDF

membranes was monitored by Ponceau S staining. Rabbit anti-Protein A, rabbit anti-Pah1 PAP (35), rabbit anti-Cho1 phosphatidylserine synthase (77), and mouse anti-phosphoglycerate kinase antibodies were used at a final concentration of 2 µg/ml. Secondary antibodies (e.g. goat anti-rabbit IgG or anti-mouse IgG) conjugated with alkaline phosphatase were used at a dilution of 1:5,000. Immune complexes were detected using the enhanced chemifluorescence immunoblotting substrate. Fluorimaging was used to acquire fluorescence signals from immunoblots, and the intensities of the images were analyzed by ImageQuant software. A standard curve was used to ensure that the immunoblot signals were in the linear range of detection.

Enzyme Assays—Protein kinase activity was measured at 30 °C by following the incorporation of radiolabeled phosphate from [γ -³²P]ATP into Pah1 (35, 37, 38, 40, 42, 78). The reaction mixture for CKII contained 20 mM Tris-HCl (pH 7.5), 10 mM MgCl₂, 50 µM [γ -³²P]ATP (2,500 cpm/pmol), 25 µg/ml Pah1, and the indicated amounts of CKII in a total volume of 20 µl. The reaction mixture for PKA contained 25 mM Tris-HCl (pH 7.5), 10 mM MgCl₂, 2 mM dithiothreitol, 100 µM [γ -³²P]ATP (3,000 cpm/pmol), 50 µg/ml Pah1, and protein kinase in a total volume of 20 µl. The reaction mixture for PKC contained 50 mM Tris-HCl (pH 7.5), 10 mM MgCl₂, 10 mM 2-mercaptoethanol, 1.7 mM CaCl₂, 500 µM phosphatidylserine, 156 µM DAG, 100 µM [γ -³²P]ATP (3,000 cpm/pmol), 50 µg/ml Pah1, and protein kinase in a total volume of 20 µl. The reaction mixture for Pho85-Pho80 contained 25 mM Tris-HCl (pH 7.5), 10 mM MgCl₂, 100 µM dithiothreitol, 100 µM [γ -³²P]ATP (3,000 cpm/

Phosphorylation of Pah1 Phosphatidate Phosphatase by CKII

TABLE 3

Plasmids used for Pah1 expression in *S. cerevisiae*

Plasmid	Relevant characteristics	Source/Reference
pRS415	Low copy <i>E. coli</i> /yeast shuttle vector with <i>LEU2</i>	Ref. 108
pGH315	<i>PAH1</i> inserted into pRS415	Ref. 35
pGH315(T170A)	<i>PAH1</i> (T170A) derivative of pGH315	This study
pGH315(T170E)	<i>PAH1</i> (T170E) derivative of pGH315	This study
pGH315(S250A)	<i>PAH1</i> (S250A) derivative of pGH315	This study
pGH315(S250D)	<i>PAH1</i> (S250D) derivative of pGH315	This study
pGH315(S313A)	<i>PAH1</i> (S313A) derivative of pGH315	This study
pGH315(S313D)	<i>PAH1</i> (S313D) derivative of pGH315	This study
pGH315(S705A)	<i>PAH1</i> (S705A) derivative of pGH315	This study
pGH315(S705D)	<i>PAH1</i> (S705D) derivative of pGH315	This study
pGH315(S814A)	<i>PAH1</i> (S814A) derivative of pGH315	This study
pGH315(S814D)	<i>PAH1</i> (S814D) derivative of pGH315	This study
pGH315(S818A)	<i>PAH1</i> (S818A) derivative of pGH315	This study
pGH315(S818D)	<i>PAH1</i> (S818D) derivative of pGH315	This study
pGH315(4A) (CKII phosphorylation sites)	<i>PAH1</i> (T170A/S313A/S705A/S818A) derivative of pGH315	This study
pGH315(4D(E)) (CKII phosphorylation sites)	<i>PAH1</i> (T170E/S313D/S705D/S818D) derivative of pGH315	This study
pGH315(6A) (CKII phosphorylation sites)	<i>PAH1</i> (T170A/S250A/S313A/S705A/S814A/S818A) derivative of pGH315	This study
pGH315(6D(E)) (CKII phosphorylation sites)	<i>PAH1</i> (T170E/S250D/S313D/S705D/S814D/S818D) derivative of pGH315	This study
pGH315(7A) (pHC204) (Pho85-Pho80 phosphorylation sites)	<i>PAH1</i> (S110A/S114A/S168A/S602A/T723A/S744A/S748A) derivative of pGH315	Ref. 35
pGH315(7D(E)) (Pho85-Pho80 phosphorylation sites)	<i>PAH1</i> (S110D/S114D/S168D/S602D/T723E/S744D/S748D) derivative of pGH315	This study
pGH315(S705A/7A)	<i>PAH1</i> (S110A/S114A/S168A/S602A/S705A/T723A/S744A/S748A) derivative of pGH315	This study
pGH315(S705D/7A)	<i>PAH1</i> (S110A/S114A/S168A/S602A/S705D/T723A/S744A/S748A) derivative of pGH315	This study
pGH315(S705D/7D(E))	<i>PAH1</i> (S110D/S114D/S168D/S602D/S705D/T723E/S744D/S748D) derivative of pGH315	This study
pGH315(4A/7A) (CKII and Pho85-Pho80 phosphorylation sites)	<i>PAH1</i> (S110A/S114A/T170A/S168A/S313A/S602A/S705A/T723A/S744A/S748A/S818A) derivative of pGH315	This study
pGH315(6A/7A) (CKII and Pho85-Pho80 phosphorylation sites)	<i>PAH1</i> (S110A/S114A/T170A/S168A/S250A/S313A/S602A/S705A/T723A/S744A/S748A/S814A/S818A) derivative of pGH315	This study

pmol), 50 μ g/ml Pah1, and the protein kinase complex in a total volume of 20 μ l. The reaction mixture for Cdc28-cyclin B contained 25 mM Tris-HCl (pH 7.5), 10 mM MgCl₂, 2 mM dithiothreitol, 20 μ M [γ -³²P]ATP (2,400 cpm/pmol), 50 μ g/ml Pah1, and protein kinase complex in a total volume of 20 μ l. The enzyme reactions were terminated by the addition of 6.7 μ l of 4 \times Laemmli sample buffer (69), resolved by SDS-PAGE, and transferred to PVDF membranes. Phosphorylated Pah1 was visualized by phosphorimaging, and the extent of phosphorylation was quantified by ImageQuant software. PAP activity was measured at 30 $^{\circ}$ C by following the release of water-soluble ³²P_i from chloroform-soluble [³²P]PA as described by Carman and Lin (73). The reaction mixture contained 50 mM Tris-HCl (pH 7.5), 1 mM MgCl₂, 0.2 mM [³²P]PA (10,000 cpm/nmol), 2 mM Triton X-100, and Pah1 protein in a total volume of 100 μ l. Nem1-Spo7 protein phosphatase activity was measured by following the release of ³²P_i from [³²P]Pah1 as described by Su *et al.* (43). The reaction mixture contained 100 mM sodium acetate (pH 5.0), 10 mM MgCl₂, 0.25 mM Triton X-100, 1 mM DTT, 25 nM [³²P]Pah1, and 0.87 ng Nem1-Spo7 protein complex in a total volume of 50 μ l. All enzyme reactions were conducted in triplicate with an average S.D. of \pm 5%. The enzyme reactions were linear with time and protein concentration. A unit of enzyme activity was defined as nmol/min unless otherwise indicated.

Preparation of Radiolabeled Substrates—The ³²P-labeled PA used for the PAP assay was enzymatically synthesized from DAG and [γ -³²P]ATP by *E. coli* DAG kinase; the radiolabeled product was separated from the substrate by TLC and then extracted from the silica gel (73). The ³²P-labeled Pah1 used for

the Nem1-Spo7 protein phosphatase assay was enzymatically synthesized from *E. coli*-expressed Pah1 and [γ -³²P]ATP by PKA (38), PKC (42), Pho85-Pho80 (37), or Cdc28-cyclin B (35). The stoichiometry of each phosphorylation reaction was determined to confirm the maximum extent of phosphorylation (43). As described previously (43), [³²P]Pah1 was purified by chromatography with Q-Sepharose or nickel-nitrilotriacetic acid-agarose and then concentrated by ultrafiltration.

Labeling and Analysis of Lipids—The steady-state labeling of lipids with [2-¹⁴C]acetate was performed as described by Morlock *et al.* (79). Lipids were extracted (80) from the radiolabeled cells and fractionated by one-dimensional TLC (81). Phosphorimaging analysis was used to identify TAG on the TLC plate, and the amount was quantified using ImageQuant software. The migration of the radiolabeled TAG was compared with that of authentic standard after exposure to iodine vapor.

Analyses of Lipid Droplets by Fluorescence Microscopy—For lipid droplet analysis, cells were grown in SC medium, stained for 30 min with 2 μ M BODIPY 493/503, washed with phosphate-buffered saline (pH 7.4), and visualized with a long pass green fluorescent protein filter. Microscopy was performed with a Nikon ECLIPSE Ni-U microscope using a 100 \times oil immersion objective.

Analyses of Data—SigmaPlot software was used for the statistical analysis of data. The *p* values <0.05 were taken as a significant difference. The enzyme kinetics module of SigmaPlot software was used to analyze kinetic data according to Michaelis-Menten and Hill equations.

Results

Phosphorylation of Pah1 by CKII—We previously showed that Pah1 is phosphorylated *in vitro* by human CKII (40). In this work, we examined its phosphorylation using a purified preparation of yeast CKII. The Pah1 expressed and purified from *E. coli* was used as a substrate free of the endogenous phosphorylations that occur in *S. cerevisiae* (33). The unphosphorylated Pah1 was incubated with yeast CKII in the presence of [γ - 32 P]ATP, and its phosphorylation was monitored by following the incorporation of the radioactive γ -phosphate. Phosphorylated Pah1 was resolved by SDS-PAGE and then detected by phosphorimaging (Fig. 2A). As described previously (40), Pah1 was also phosphorylated by human CKII (Fig. 2A). Phosphoamino acid analysis showed that Pah1 is phosphorylated at both serine and threonine residues by yeast or human CKII (Fig. 2B). Phosphopeptide mapping analysis showed the identical patterns of phosphopeptide separation, indicating that yeast and human CKII enzymes phosphorylate Pah1 on the same sites (Fig. 2C). To conserve on the yeast CKII enzyme that had to be purified, we used the commercially prepared human CKII enzyme in further extensive phosphopeptide mapping experiments to identify the sites of phosphorylation (see below).

That Pah1 is a *bona fide* substrate of yeast CKII was shown by the kinase activity that was dependent on the time of reaction and the amount of protein kinase (Fig. 3, A and B, respectively). In addition, yeast CKII followed saturation kinetics with respect to the concentrations of Pah1 and ATP (Fig. 3, C and D, respectively). The K_m value for Pah1 is similar to that of the Pho85-Pho80 and Cdc28-cyclin B protein kinases and is 1.9- and 3.2-fold lower, respectively, when compared with those of PKA and PKC (Table 4). The K_m value for ATP of the CKII enzyme was also within the range of other protein kinases that phosphorylate Pah1 (Table 4). At the point of maximum phosphorylation, CKII catalyzed the incorporation of 2 mol of phosphate/mol of Pah1, a stoichiometry higher than that shown for PKA, PKC, and Cdc28-cyclin B but lower than that for Pho85-Pho80 (Table 4).

Effects of the CKII Phosphorylation of Pah1 on PAP Activity, 20S Proteasomal Degradation, and Nem1-Spo7 Protein Phosphatase Activity—The effect of CKII phosphorylation on Pah1 PAP activity was examined as a function of the PA surface concentration. As described previously (10), the unphosphorylated Pah1 exhibited positive cooperative (Hill number = 2.5) kinetics with respect to the PA concentration ($K_m = 2$ mol %) (Fig. 4A). The CKII phosphorylation of Pah1 did not have a significant effect on the K_m or cooperativity for PA but had a small (13%) inhibitory effect on the V_{max} of the reaction (Fig. 4A).

Pah1 is subject to the proteasome-mediated degradation in the stationary phase of growth (44). The degradation, which occurs by the 20S proteasome via a ubiquitin-independent mechanism, is regulated by phosphorylation (45). For example, the phosphorylations of Pah1 by Pho85-Pho80 and PKA prevent it from degradation by the 20S proteasome, whereas its phosphorylation by PKC stimulates the proteasomal degradation (45). Accordingly, we questioned whether the CKII phosphorylation of Pah1 affects its 20S proteasomal degradation. The *E. coli*-expressed Pah1 was first phosphorylated by yeast

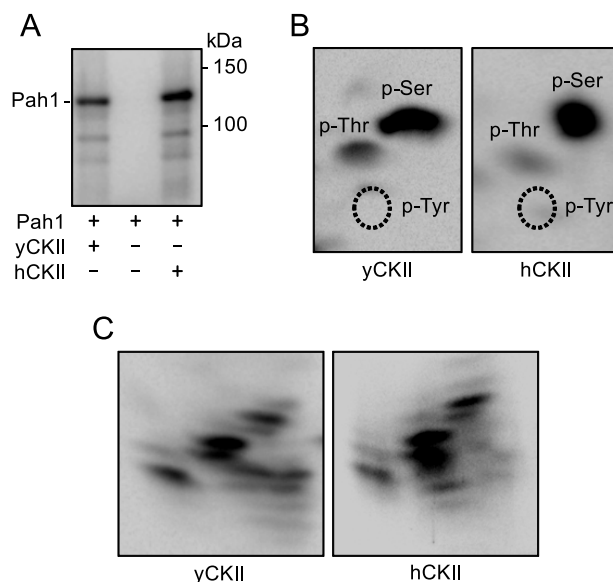


FIGURE 2. CKII phosphorylates Pah1 on serine and threonine residues. A, 0.5 μ g of Pah1 was phosphorylated by 3 units of yeast CKII (*yCKII*) or 10 units of human CKII (*hCKII*) with 50 μ M [γ - 32 P]ATP (2,500 cpm/pmol) for 10 min. Following the kinase reactions, Pah1 was separated from ATP and CKII by SDS-PAGE and was subjected to phosphorimaging analysis. B and C, 32 P-labeled Pah1 in the polyacrylamide gel was transferred to the PVDF membrane and then incubated with HCl or with L-1-tosylamido-2-phenylethyl chloromethyl ketone-treated trypsin. The phosphoamino acids produced by the acid hydrolysis were separated on cellulose TLC plates by two-dimensional electrophoresis (B), whereas the phosphopeptides produced by the enzyme digestion were separated on cellulose TLC plates by electrophoresis (from left to right) in the first dimension and by chromatography (from bottom to top) in the second dimension (C). The positions of Pah1, molecular mass standards, and the standard phosphoamino acids phosphoserine (*p-Ser*), phosphothreonine (*p-Thr*), and phosphotyrosine (*p-Tyr*) (dotted lines) are indicated. The data shown in the figure are representative of three experiments.

CKII and then incubated with the purified 20S proteasome. As described previously (45), the unphosphorylated Pah1 was degraded by the 20S proteasome in a time-dependent manner. The CKII-phosphorylated Pah1 was also degraded almost at the same rate by the 20S proteasome (Fig. 4B), indicating that the phosphorylation of Pah1 by CKII has no significant effect on its proteasomal degradation.

The Nem1-Spo7 protein phosphatase complex (34) dephosphorylates Pah1 (15, 33, 43) to facilitate its interaction with the nuclear/ER membrane (36, 39, 41) and to stimulate its PAP activity that is attenuated through the phosphorylations by Pho85-Pho80 and PKA (37, 38, 43). Here, we examined whether the CKII-phosphorylated Pah1 is dephosphorylated by Nem1-Spo7. Indeed, the CKII-phosphorylated Pah1 was a substrate for Nem1-Spo7 (Fig. 5). It was equally as good as the PKA-phosphorylated substrate and was 3.7- and 1.8-fold better than the PKC-phosphorylated and Cdc28-cyclin B-phosphorylated substrates, respectively. However, the CKII-phosphorylated Pah1 was 3.8-fold worse than the substrate phosphorylated by Pho85-Pho80.

Prephosphorylation of Pah1 by PKA or PKC Reduces Subsequent Phosphorylation by CKII, and Prephosphorylation by CKII Reduces Subsequent Phosphorylation by PKA—The rationale for using unphosphorylated Pah1 as a substrate for CKII was to eliminate potential effects of prior phosphorylations by other protein kinases. In this series of experiments, we

Phosphorylation of Pah1 Phosphatidate Phosphatase by CKII

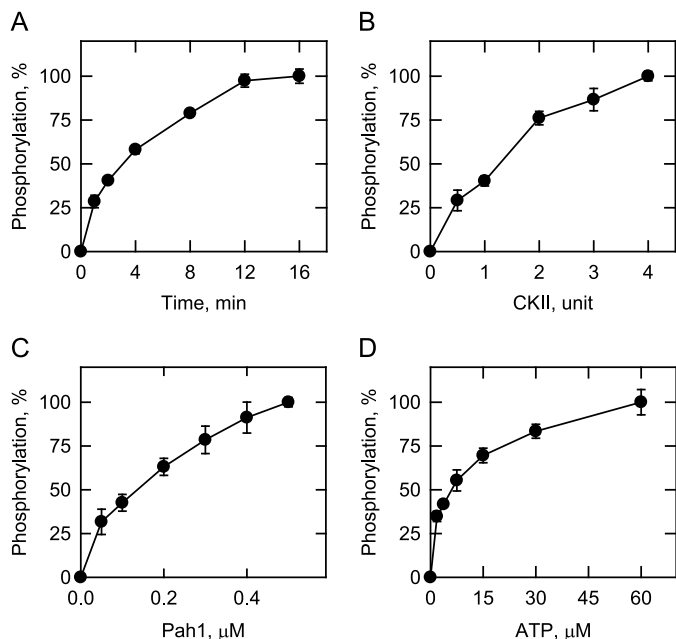


FIGURE 3. Pah1 is a bona fide substrate of CKII. Phosphorylation of Pah1 by yeast CKII was measured by following the incorporation of the radiolabeled phosphate from [γ - 32 P]ATP into purified recombinant Pah1 under standard assay conditions by varying reaction time (A), the amount of yeast CKII (B), and the concentrations of Pah1 (C) and ATP (D). After the kinase reactions, the samples were subjected to SDS-PAGE and then subjected to phosphorimaging analysis. The relative amounts of phosphate incorporated into Pah1 were quantified by ImageQuant software. The data shown in A–D are the averages of three experiments \pm S.D. (error bars).

TABLE 4
Kinetic properties of protein kinases that phosphorylate Pah1

Protein kinase	Pah1 K_m	ATP K_m	Stoichiometry	Reference
	μM	μM	$\text{mol phosphate/mol Pah1}$	
Pho85-Pho80	0.25	3.7	4.0	Ref. 37
Cdc28-cyclin B	0.21	5.8	0.8	Ref. 35
PKA	0.44	4.4	1.0	Ref. 38
PKC	0.75	4.5	0.8	Ref. 42
CKII	0.23	5.5	2.0	This study

examined whether the phosphorylation of Pah1 by PKA, PKC, Pho85-Pho80, or Cdc28-cyclin B affects its subsequent phosphorylation by CKII. Pah1 was individually phosphorylated by various protein kinases with unlabeled ATP and then phosphorylated by yeast CKII with [γ - 32 P]ATP. Compared with Pah1 that was not subjected to prephosphorylation, Pah1 phosphorylated by PKA or PKC showed a reduction in its phosphorylation by CKII of 23 and 29%, respectively (Fig. 6A). Coincidentally, three serine residues (*i.e.* Ser-677, Ser-773, and Ser-788) of Pah1 are common target sites for PKA and PKC (38, 42) (Fig. 1B). The phosphorylation-deficient alanine mutations of the five PKA sites (38) or the four PKC sites (42) removed the negative effect of the Pah1 prephosphorylation by PKA or PKC on its subsequent phosphorylation by CKII (Fig. 6A). The prephosphorylation of Pah1 by Pho85-Pho80 or Cdc28-cyclin B did not influence its subsequent phosphorylation by CKII (Fig. 6A). In a reciprocal set of experiments, Pah1 was first phosphorylated with unlabeled ATP by yeast CKII and then phosphorylated with [γ - 32 P]ATP by PKA, PKC, Pho85-Pho80, or Cdc28-cyclin B. The only reaction affected by the prephosphorylation was that of PKA; the prephosphorylation of Pah1 by CKII caused a

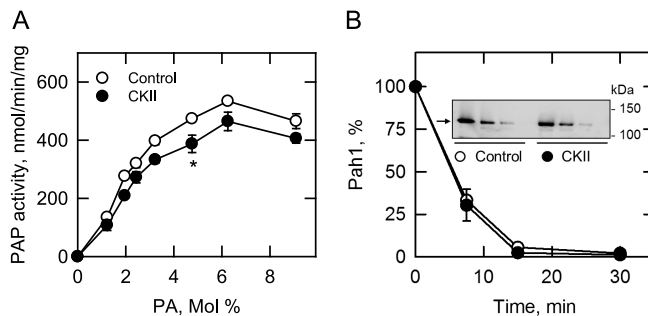


FIGURE 4. Effects of CKII phosphorylation of Pah1 on PAP activity and on the 20S proteasomal degradation of Pah1. Pah1 was phosphorylated by yeast CKII with unlabeled ATP. A, following the phosphorylation, the phosphorylated and unphosphorylated (*control*) forms of the enzyme were measured for PAP activity as a function of the surface concentration of PA. By maintaining the molar concentration of PA at 0.2 mM, the molar concentration of Triton X-100 was varied to obtain the indicated surface concentrations of PA. B, the phosphorylated and unphosphorylated (*control*) forms of Pah1 were incubated with the 20S proteasome for various periods of time. Following the incubations, Pah1 samples were subjected to SDS-PAGE and were detected by immunoblotting with anti-Pah1 antibodies. The relative amounts of Pah1 were quantified using ImageQuant software. The immunoblot shown in the inset of B is representative of three experiments. The positions of Pah1 (arrow) and the molecular mass standards are indicated. *, $p < 0.05$ versus control.

36% reduction in its subsequent phosphorylation by PKA (Fig. 6B). The phosphorylation-deficient alanine mutations of four CKII sites (*i.e.* T170A/S313A/S705A/S818A; see below) obviated the inhibitory effect of the prephosphorylation by CKII (Fig. 6B).

CKII Phosphorylates Pah1 on Thr-170, Ser-250, Ser-313, Ser-705, Ser-814, and Ser-818—The strategy used to identify the CKII phosphorylation sites included mass spectrometry, phosphopeptide mapping, and phosphoamino acid analyses of wild type and mutant forms of Pah1. In our study by mass spectrometry, the *E. coli*-expressed wild type Pah1 was shown to be phosphorylated by human CKII on Ser-250 and Ser-814. This analysis also identified a phosphopeptide that contained Ser-704, Ser-705, and Ser-711, but it was unclear which serine residue(s) was phosphorylated. The five serine residues were individually changed to an alanine residue, and the mutant enzymes were expressed and purified from *E. coli*; they were phosphorylated by CKII and then subjected to proteolytic digestion and phosphopeptide mapping. This analysis showed that Ser-705 was the target of phosphorylation; a phosphopeptide present in the map of wild type Pah1 was missing in the map of the S705A mutant (Fig. 7C). The mutagenesis of Ser-250 or Ser-814 did not cause the loss of any major phosphopeptide, indicating that the serine residues are not major sites of phosphorylation (Fig. 7C). The multiple phosphopeptides that were still present in the map of the S705A mutant indicated that additional approaches were needed to identify major CKII target sites in Pah1.

To narrow down the regions of the CKII-phosphorylated Pah1, a series of its truncations (Fig. 7A) were phosphorylated by the protein kinase and then subjected to phosphopeptide mapping analysis (Fig. 7B). Compared with wild type Pah1, Pah1(1–821) showed no loss of phosphopeptide. In contrast, Pah1(1–700) and Pah1(1–646) showed the loss of two identical phosphopeptides, indicating that at least two CKII phosphory-

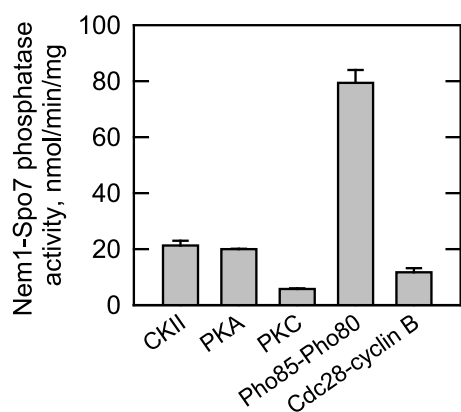


FIGURE 5. Nem1-Spo7 protein phosphatase utilizes CKII-phosphorylated Pah1 as a substrate. Purified unphosphorylated Pah1 was phosphorylated by CKII, PKA, PKC, Pho85-Pho80, or Cdc28-cyclin B with $[\gamma\text{-}^{32}\text{P}]\text{ATP}$. The ^{32}P -labeled Pah1 was purified and used as a substrate (25 nM) for the Nem1-Spo7 protein phosphatase. The data shown are means \pm S.D. (error bars) from triplicate enzyme determinations.

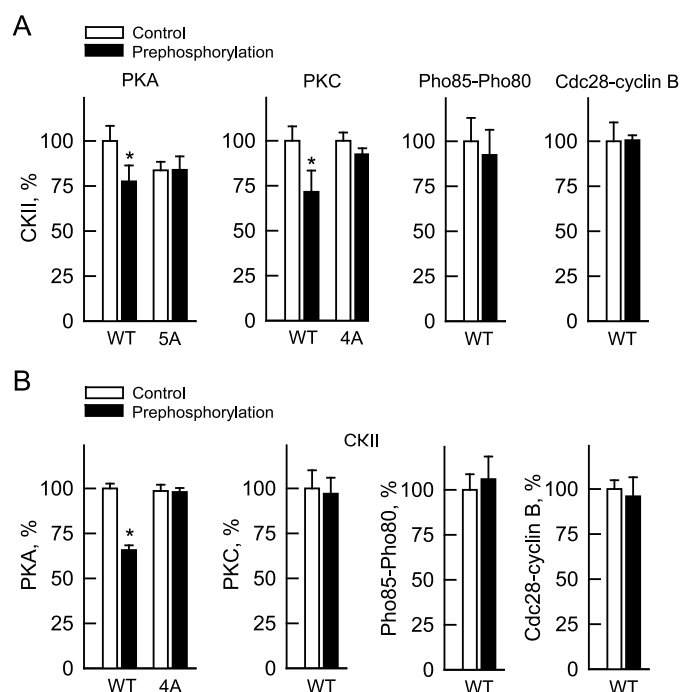


FIGURE 6. Prephosphorylation of Pah1 by PKA or PKC reduces subsequent phosphorylation by CKII, and prephosphorylation by CKII reduces subsequent phosphorylation by PKA. Wild type and the indicated phosphorylation site mutants were expressed and purified from *E. coli*. *A*, unphosphorylated Pah1 was prephosphorylated by PKA, PKC, Pho85-Pho80, or Cdc28-cyclin B with unlabeled ATP. The prephosphorylated Pah1 was then phosphorylated by yeast CKII with $[\gamma\text{-}^{32}\text{P}]\text{ATP}$. *B*, unphosphorylated Pah1 was prephosphorylated by yeast CKII with unlabeled ATP. The prephosphorylated Pah1 was then phosphorylated by PKA, PKC, Pho85-Pho80, or Cdc28-cyclin B with $[\gamma\text{-}^{32}\text{P}]\text{ATP}$. Following the kinase reactions, Pah1 was separated from labeled ATP by SDS-PAGE and subjected to phosphorimaging and ImageQuant analyses. The amount of the phosphorylated wild type Pah1 was set at 100%. The control for these experiments was Pah1 that was not subjected to prephosphorylation. The data reported are the average of three independent experiments \pm S.D. (error bars). 5A and 4A (in *A*), PKA and PKC phosphorylation site mutations, respectively. 4A (in *B*), CKII phosphorylation site mutations. *, $p < 0.05$ versus control.

lation sites are located in residues 701–821. In addition, Pah1(235–752) showed the loss of one phosphopeptide that is also missing in Pah1(1–700) and Pah1(1–646), indicating that one phosphorylation site is located in residues 753–821.

Accordingly, another phosphorylation site was expected to be located between residues 701 and 752, and additional phosphorylation sites were expected to be located between residues 235 and 646. As described above, Ser-705 was identified as a CKII phosphorylation site by mass spectrometry and phosphopeptide mapping.

Phosphoproteome analyses (82, 83) indicated that Ser-311, Ser-327, Ser-475, and Ser-511, which are contained within residues 235–646, are sites of phosphorylation, but the protein kinases involved are not known. Phosphopeptide mapping analysis of the alanine mutants for each of these serine residues indicated that they are not major target sites for CKII. The analyses of the Pah1 sequence by the NetPhosK (84) and KinasePhos (85) algorithms indicated that it contains 14 putative CKII target sites (*i.e.* Ser-250, Ser-254, Ser-311, Ser-313, Thr-315, Thr-319, Ser-320, Ser-327, Thr-364, Ser-397, Ser-511, Thr-517, Thr-553, and Ser-613) within the residues 235–646. The phosphopeptide mapping analysis of the alanine mutants for each of these serine residues showed that Ser-313 was responsible for two phosphopeptides generated from the CKII-phosphorylated Pah1 (Fig. 7C).

We next sought to identify the CKII phosphorylation sites in the residues 753–821. This region contains three residues (*i.e.* Ser-814, Thr-816, and Ser-818) that are within the consensus motif for CKII. Two of these sites (*e.g.* Ser-814 and Ser-818) were previously identified by mass spectrometry of purified Pah1 (33), whereas all three sites have been identified in various phosphoproteomic analyses (82, 83, 86, 87). As indicated above, the phosphopeptide map of the S814A mutant was indistinguishable from that of the wild type enzyme. Of the remaining two sites, only the S818A mutation caused the loss of a phosphopeptide in the map (Fig. 7C). The phosphopeptide map of the S250A/S705A/S814A triple mutant showed only the loss of the phosphopeptide ascribed to Ser-705 (Fig. 7C). The map of the S313A/S705A double mutant showed the loss of the phosphopeptides ascribed to Ser-313 and Ser-705, and the only major peptide remaining in this map was ascribed to Ser-818 (Fig. 7C).

Pah1 was shown to be phosphorylated by CKII on a threonine residue(s) (Figs. 2B and 7D). However, no noticeable difference was shown in the phosphopeptide maps of the wild type and the alanine mutants for the threonine residues (*i.e.* T170A, T176A, T315A, T319A, T364A, T517A, T553A, and T816A) that were previously identified by phosphoproteome studies (82, 83, 86) or are located within a consensus CKII site (84, 85). This may be due to the fact that the extent of threonine phosphorylation was much lower than that of serine phosphorylation (Figs. 2B and 7D). Accordingly, we looked for a mutation(s) that affected the phosphoamino acid profile of Pah1. The phosphoamino acid analysis of all of the individual threonine-to-alanine mutants showed that only Thr-170 was the target site of CKII (Fig. 7D).

We examined the effects of phosphorylation site mutations individually or in combination on the extent of Pah1 phosphorylation by CKII (Fig. 8). Ser-313, Ser-705, Ser-814, and Ser-818 are in the context of the optimum recognition motif for CKII (60). The alanine mutations of these sites, with the exception of S814A, affected the phosphopeptide map of Pah1 and caused a

Phosphorylation of Pah1 Phosphatidate Phosphatase by CKII

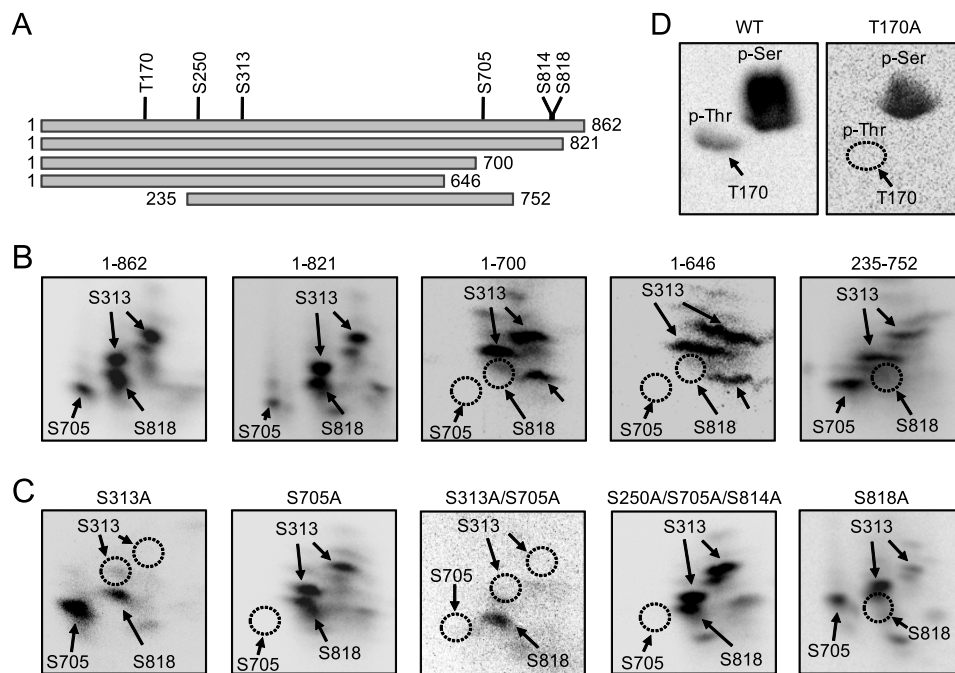


FIGURE 7. Phosphopeptide mapping and phosphoamino acid analyses of Pah1 mutants identify its CKII phosphorylation sites. *A*, the diagram shows full-length and truncated forms of Pah1 used for phosphorylation and phosphopeptide mapping analysis. The positions of the identified phosphorylation sites are indicated in full-length Pah1. *B–D*, wild type Pah1 and its truncations and phosphorylation site mutants were expressed and purified from *E. coli*. Samples (1 μ g) of the indicated forms of Pah1 were phosphorylated by 10 units of human CKII with 50 μ M [γ - 32 P]ATP (2,500 cpm/pmol) for 10 min. The phosphorylated samples were resolved by SDS-PAGE and transferred to a PVDF membrane. The 32 P-labeled Pah1 from the PVDF membrane was subjected to phosphopeptide mapping (*B* and *C*) or phosphoamino acid (*D*) analyses as described in the legend to Fig. 2. The identity of the phosphorylation sites in the radioactive phosphopeptides or phosphothreonine of wild type Pah1 was determined from the phosphopeptide or phosphoamino acid maps of the phosphorylation site mutant enzymes. The positions of the phosphopeptides or phosphothreonine that were absent in the mutant enzymes (indicated by the dotted line circles) but were present in wild type Pah1 are indicated. The unlabeled arrow in the phosphopeptide maps of the truncations of 1–700 and 1–646 points to the unidentified phosphopeptide that is more heavily labeled when compared with that found in the other maps. This figure does not show the negative results of all phosphopeptide mapping and phosphoamino acid analysis experiments performed on the mutants (see Table 2) discussed. The data shown are representative of three independent experiments.

significant decrease in the phosphorylation by 48, 28, and 25%, respectively. Although S814A did not affect the phosphopeptide map of Pah1, the mutation caused a 13% decrease in phosphorylation. The alanine mutations for Thr-170 and Ser-250, which are in the less optimum recognition motif for CKII, did not affect the phosphopeptide map of Pah1 and caused only small decreases in the phosphorylation by 6 and 1%, respectively. The 4A (T170A/S313A/S705A/S818A) and 6A (T170A/S250A/S313A/S705A/S814A/S818A) mutations, which include the major and minor phosphorylation site mutations, caused a greater reduction of Pah1 phosphorylation by 91 and 93%, respectively, indicating that the mutational effects are additive. The low level of phosphorylation shown by the 6A mutant suggests that a minor site(s) whose identity is yet unknown is involved in the phosphorylation of Pah1. These results, along with those of the phosphopeptide mapping analyses, showed that the phosphorylation efficiency on each site was different. For example, Ser-313 was the most heavily phosphorylated residue, whereas Ser-250 was the least phosphorylated residue. The phosphopeptide mapping results also showed that a single site mutation (e.g. S313A) not only abolishes the target phosphorylation but also affects the extent of phosphorylation on other sites (e.g. Ser-705) (Fig. 7C). We also noted in the truncation analysis (e.g. 1–700 and 1–646) that a major phosphopeptide appeared to the right of the phosphopeptide ascribed to Ser-818 (Fig. 7B, unlabeled arrow). The

identity of this phosphopeptide was not determined. The complex nature of these phosphorylations suggests that the phosphorylation of one site affects the phosphorylation of another site. Thus, the hierarchical phosphorylation (88) may provide an explanation as to why the stoichiometry of 2 mol of phosphate/mol of Pah1 is lower than that expected from six sites of phosphorylation.

Effects of CKII Phosphorylation Site Mutations on the Abundance, Location, and Physiological Function of Pah1—A series of serine/threonine-to-alanine and -aspartate/glutamate mutations (Table 3) were constructed for the CKII phosphorylation sites in order to examine the physiological effects of phosphorylation-deficient/mimicking Pah1. The mutant alleles of *PAH1* were expressed in *pah1* Δ or *pah1* Δ *nem1* Δ cells from a low copy plasmid. The rationale for expressing the mutant Pah1 in the *nem1* Δ background was to assess the dependence of its function on Nem1-Spo7 protein phosphatase and to assess the phosphorylation site mutations in a genetic background that favors the phosphorylation of non-mutated sites in Pah1. Immunoblot analysis of cell extracts showed that none of the CKII phosphorylation site mutations, individually or in combination, affected the abundance of Pah1. In addition, its abundance was not affected by mutations (e.g. *cka1* Δ , *cka2* Δ , *ckb1* Δ , or *ckb2* Δ) in any of the CKII subunits.

The subcellular location of Pah1 was examined in cells expressing the mutant alleles of *PAH1* for Thr-170, Ser-313,

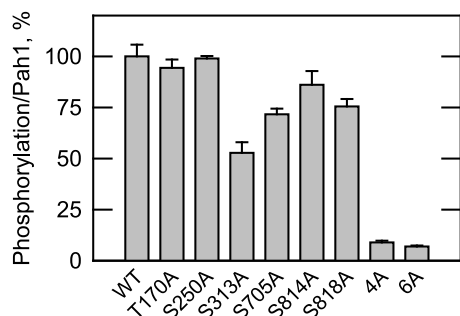


FIGURE 8. CKII phosphorylation site mutations reduce the phosphorylation of Pah1. Wild type and the indicated Pah1 phosphorylation site mutants were expressed and purified from *E. coli*. The Pah1 enzymes were phosphorylated by 3 units of yeast CKII with 50 μM [γ - ^{32}P]ATP (2,500 cpm/pmol) for 10 min. Following the kinase reaction, Pah1 was separated from labeled ATP by SDS-PAGE and subjected to phosphorimaging and ImageQuant analyses. The amount of the phosphorylated wild type enzyme was set at 100%. The data reported are the average of three independent experiments \pm S.D. (error bars). 4A and 6A, CKII phosphorylation site mutations.

Ser-705, and Ser-818. Mutations for Ser-250 and Ser-814 were not included in this analysis because they did not have a major effect on the phosphorylation of Pah1. The S705A mutant, expressed in either *pah1* Δ or *pah1* Δ *nem1* Δ cells, showed a 2-fold increase in membrane association when compared with the wild type control (Fig. 9A). Because the alanine mutations of the seven sites (*i.e.* 7A mutations) phosphorylated by Pho85-Pho80 (Fig. 1B) cause an increase in the association of Pah1 with the membrane (35), we questioned what effect the S705A mutation has on this regulation. In *pah1* Δ or *pah1* Δ *nem1* Δ cells, the combination of the S705A and 7A mutations showed no significant increase in the membrane association of Pah1 when compared with S705A or 7A (Fig. 9A). Except for S705A, other serine/threonine-to-alanine (Fig. 9A) or serine/threonine-to-aspartate/glutamate (Fig. 9B) mutations for the CKII phosphorylation sites showed little effect on the subcellular localization of Pah1.

As described previously (10, 15, 89), cells lacking Pah1 (*i.e.* *pah1* Δ mutant) exhibited a temperature-sensitive phenotype (Fig. 10A) that reflects the important role of PAP activity in cell physiology (10). The temperature sensitivity of the *pah1* Δ mutant, which expresses the Nem1-Spo7 phosphatase complex, was complemented by the *PAH1* alleles with alanine or aspartate/glutamate mutations, alone or in combination, for the CKII phosphorylation sites (Fig. 10A). As described previously (35), *pah1* Δ *nem1* Δ mutant cells, which lack both Pah1 and the Nem1-Spo7 phosphatase complex, are also temperature-sensitive for growth (Fig. 10B). That this phenotype was poorly complemented by wild type *PAH1* (Fig. 10B) reflects the importance of the Nem1-Spo7 phosphatase in Pah1 function (15, 33, 35). Moreover, the alanine mutations, alone or in combination, of the CKII sites did not have a major suppressive effect over that shown for the wild type enzyme (Fig. 10B).

Pah1-7A, which is defective in phosphorylation by Pho85-Pho80, bypasses the requirement of the Nem1-Spo7 phosphatase complex and complements the temperature-sensitive phenotype of the *pah1* Δ *nem1* Δ mutant (35, 38) (Fig. 10B). The molecular basis for this complementation is that the phosphorylation-deficient 7A mutations allow Pah1 to directly interact with the membrane as a functional enzyme in the absence of

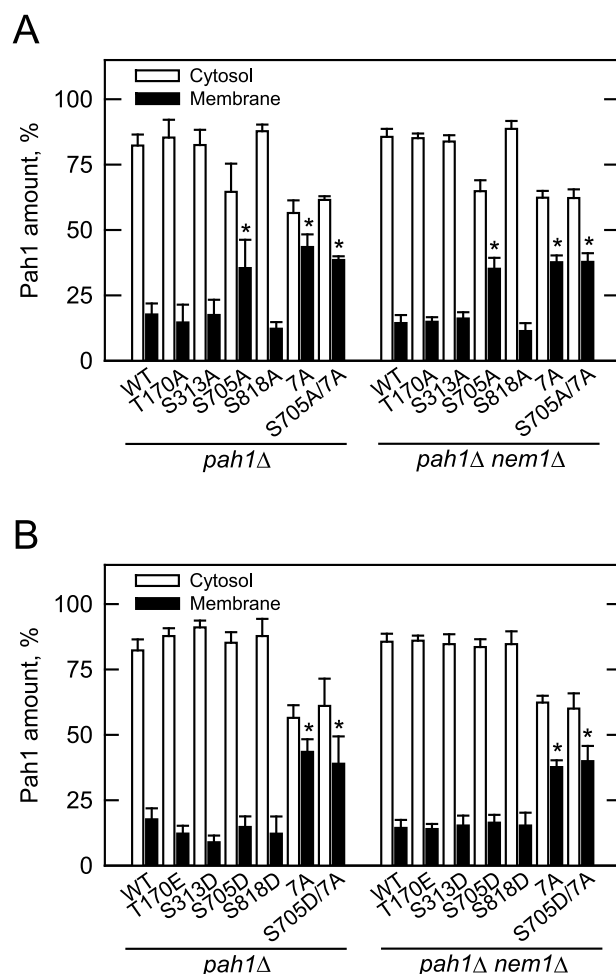


FIGURE 9. Effects of the CKII and Pho85-Pho80 phosphorylation site mutations on the membrane localization of Pah1. The indicated wild type and phosphorylation site mutant forms (A, alanine; B, aspartate/glutamate) of Pah1 were expressed in *pah1* Δ and *pah1* Δ *nem1* Δ cells. Cell extracts were prepared from late exponential phase cells ($A_{600} \sim 0.8$) and fractionated into the cytosolic and membrane fractions by centrifugation. The membrane fraction was resuspended in the same volume of the cytosolic fraction, and equal volumes of the fractions were subjected to immunoblot analysis with anti-Pah1, anti-Pgk1 (cytosol marker), and anti-Cho1 (ER marker) antibodies. As described previously (105), the immunoblot analysis for the marker proteins indicated highly enriched cytosolic and membrane fractions. The relative amounts of Pah1 in the cytosolic and membrane fractions were determined by ImageQuant analysis. Each data point represents the average of four experiments \pm S.D. (error bars). The data points for the wild type control and 7A mutant expressed in either *pah1* Δ or *pah1* Δ *nem1* Δ in A and B are the same for the purpose of comparison. 7A, Pho85-Pho80 phosphorylation site mutations. *, $p < 0.05$ versus control.

Nem1-Spo7 phosphatase activity (33, 35, 36, 40). Because the CKII phosphorylation-deficient S705A mutation affected the relative amounts of Pah1 in the cytosolic and membrane fractions (Fig. 9A), we examined the temperature-sensitive phenotype of the *pah1* Δ and *pah1* Δ *nem1* Δ mutants expressing Pah1 with serine-to-alanine/aspartate mutations in Ser-705 in combination with the 7A mutations. Strikingly, the S705D mutation eliminated the ability of the 7A mutations to complement the temperature sensitivity of the *pah1* Δ mutant, but only when the Nem1-Spo7 phosphatase complex was present (Fig. 10A, *bottom*). In contrast, the S705D mutation did not interfere with the ability of the 7A mutations to complement the temperature sensitivity when Nem1-Spo7 was absent (Fig. 10B, *bottom*). The

Phosphorylation of *Pah1* Phosphatidate Phosphatase by CKII

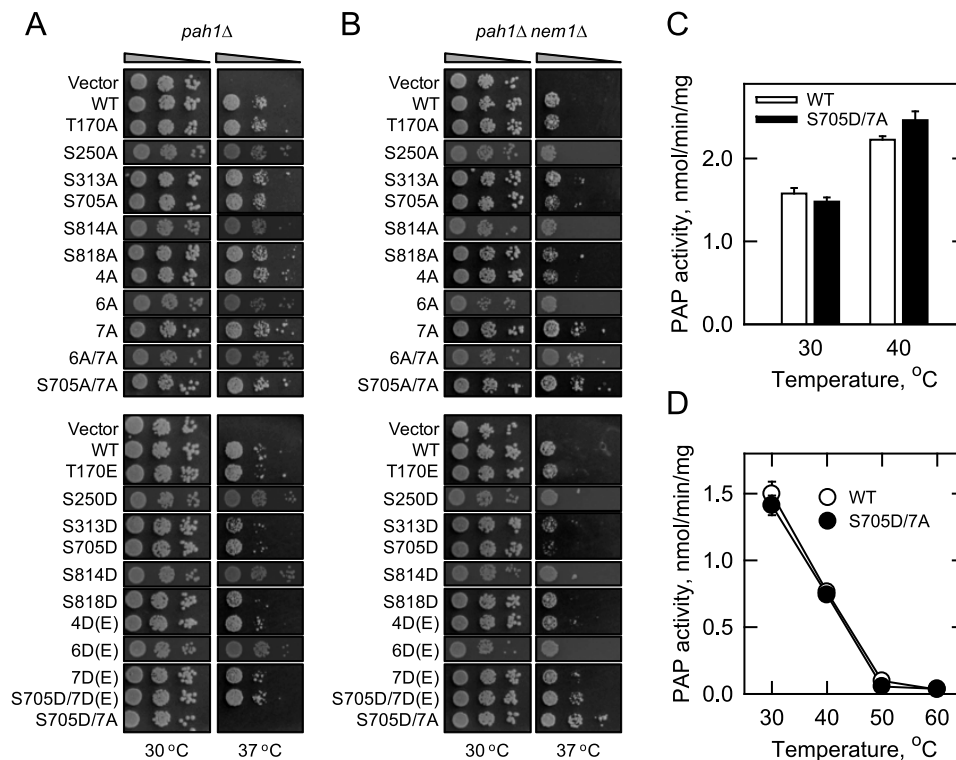


FIGURE 10. Effects of CKII and Pho85-Pho80 phosphorylation site mutations on the complementation of the *pah1Δ* temperature-sensitive phenotype and on PAP activity and stability in response to temperature. The indicated wild type and phosphorylation site mutant forms of Pah1 were expressed in the *pah1Δ* (A) and *pah1Δ nem1Δ* (B) mutants. The transformants were grown to stationary phase in SC-Leu medium at 30 °C; serial dilutions (10-fold) of the cells were spotted onto SC-Leu agar plates and incubated at 30 or 37 °C for 3–4 days. The data are representative of three independent experiments. 4A, 4D(E), 6A, and 6D(E), CKII phosphorylation site mutations; 7A and 7D(E), Pho85-Pho80 phosphorylation site mutations. C and D, cell extracts were prepared from *pah1Δ app1Δ dpp1Δ lpp1Δ* mutant cells expressing the wild type Pah1 and S705D/7A mutant enzymes. C, PAP activity was measured at the indicated temperatures for 20 min in a temperature-controlled water bath. D, samples were first incubated for 20 min at the indicated temperatures. After incubation, the samples were cooled in an ice bath for 10 min to allow for enzyme renaturation, and PAP activity was then measured for 20 min at 30 °C. The data shown are means \pm S.D. (error bars) from triplicate enzyme determinations.

effect of the S705A/7A mutations expressed in *pah1Δ* (Fig. 10A) or *pah1Δ nem1Δ* (Fig. 10B) cells was the same as that governed by the 7A mutations alone.

Because temperature sensitivity of the *pah1Δ* mutant (10, 15, 89) has been ascribed to the loss of Pah1 PAP activity (10, 16), we questioned whether the Pah1-S705D/7A mutant enzyme is temperature-sensitive at 37 °C. To address this question, the Pah1-S705D/7A mutant enzyme was expressed in the *pah1Δ app1Δ dpp1Δ lpp1Δ* quadruple mutant, and the PAP activity was measured at 30 and 40 °C. The quadruple mutant was used for this experiment to eliminate interference from the promiscuous lipid phosphate phosphatase activities imparted by the *APP1* (90, 91), *DPP1* (92), and *LPP1* (93) gene products. The Pah1 PAP activity in wild type cells at 40 °C was greater than that at 30 °C, and the level of PAP activity at 40 °C was not affected by the S705D/7A mutations (Fig. 10C). Moreover, the temperature stability profile of the Pah1 S705D/7A mutant enzyme was indistinguishable from the wild type control (Fig. 10D).

Pah1 has its greatest effect on lipid synthesis in the stationary phase of growth, when the synthesis of TAG occurs at the expense of membrane phospholipids (10, 17, 18). Accordingly, we examined the effects of the CKII phosphorylation-deficient/mimicking mutations on TAG levels in stationary phase cells. As described previously (35), expression of wild type Pah1 in *pah1Δ nem1Δ* mutant cells that lack the Nem1-Spo7 phosphatase

showed a reduction (~70%) in the amount of TAG, but the expression of the Pah1-7A mutant complemented this phenotype (Fig. 11). The TAG content of the *pah1Δ nem1Δ* mutant expressing the 7A mutant enzyme was 3.5-fold higher than that of cells expressing the wild type enzyme. Unlike the Pho85-Pho80 site 7A mutations, none of the alanine mutations for the CKII sites complemented the loss of the Nem1-Spo7 phosphatase complex (Fig. 11A). Also, the CKII phosphorylation-deficient 4A mutations or the phosphorylation mimicking S705D mutation did not affect the 7A-mediated complementation of this phenotype (Fig. 11). Unexpectedly, the S705D mutation in combination with the 7A mutations caused a significant increase (70%) in the TAG content of *pah1Δ* mutant cells (Fig. 11A), the same cells where the S705D/7A mutations caused a lethal phenotype at 37 °C (Fig. 10A).

Because the S705D/7A mutations caused a significant increase in TAG content for stationary phase cells, we questioned what effect the mutations have on cytoplasmic lipid droplets. As described previously (17, 19), wild type cells had ~10 lipid droplets/cell (Fig. 12A). However, about 10% of the cells expressing the Pah1-S705D/7A contained about twice as many lipid droplets when compared with the wild type control cells (Fig. 12A). The number of lipid droplets/cell was not affected by the S705D or 7A mutations alone. This phenotype was growth phase-dependent; the population of cells with an excess in lipid droplet number increased from 2% in exponen-

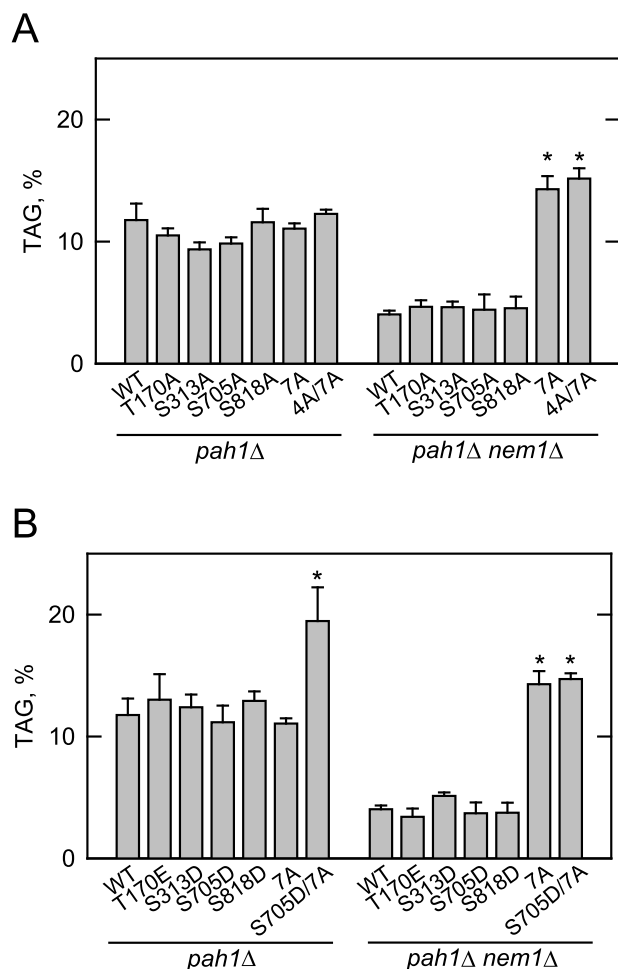


FIGURE 11. TAG synthesis is affected by the CKII phosphorylation state of Pah1 at Ser-705 in combination with its 7A mutations for the Pho85-Pho80 phosphorylation sites. The indicated wild type and phosphorylation site alanine (A) or aspartate/glutamate (B) mutant forms of Pah1 were expressed in *pah1Δ* and *pah1Δ nem1Δ* cells. Cultures were grown to the stationary phase ($A_{600} \sim 3$) in the medium containing $[2-^{14}\text{C}]$ acetate ($1 \mu\text{Ci/ml}$) to label lipids. The lipids were extracted and separated by one-dimensional TLC, and the phosphor images were subjected to ImageQuant analysis. The percentage shown for TAG was normalized to the total ^{14}C -labeled chloroform-soluble fraction. Each data point represents the average of three experiments \pm S.D. (error bars). The data points for the wild type control and 7A mutant expressed in either *pah1Δ* or *pah1Δ nem1Δ* in A and B are the same for the purpose of comparison. 4A and 7A, CKII and Pho85-Pho80 phosphorylation site mutations, respectively. *, $p < 0.05$ versus control.

tial phase (12-h growth) to 10% in stationary phase (60-h growth) (Fig. 12B).

Discussion

PAP plays a major role in regulating the balance between the synthesis of TAG and membrane phospholipids from the PA node in lipid metabolism (2–8). Efforts to understand how PAP is regulated are clearly warranted, given its important role in lipid metabolism as well as its impact on various aspects of cell physiology (2, 3, 6, 8, 13, 14). As one of the most highly regulated enzymes in yeast lipid metabolism, Pah1 PAP is controlled at the transcriptional (18, 25) and biochemical (15, 30–45) levels. In particular, the phosphorylation/dephosphorylation of Pah1 controls its localization, stability/degradation, and PAP activity (33, 35–38, 41–43). The mechanistic understanding of the

posttranslational regulation of Pah1 has been facilitated through analyses of its phosphorylation by Pho85-Pho80 (37), Cdc28-cyclin B (35), PKA (38), and PKC (42) as well as through analyses of its dephosphorylation by the Nem1-Spo7 protein phosphatase (43). In this work, we have established that Pah1 is a substrate for phosphorylation by CKII by identifying its six Ser/Thr residues as phosphorylation sites (Fig. 1B). By mutational analysis of the CKII sites, we discovered that the phosphorylation of Pah1 on Ser-705, in conjunction with its dephosphorylation on the Pho85-Pho80 sites, regulates its role in TAG synthesis.

The effects of the CKII phosphorylation of Pah1 differed from those of its phosphorylation by other protein kinases that phosphorylate the enzyme. The phosphorylations by Pho85-Pho80 (37) and PKA (38) have a relatively strong inhibitory effect on PAP activity, whereas the phosphorylation by CKII had only a weak inhibitory effect on activity. The phosphorylation by PKC (42) has a small stimulatory effect on PAP activity, whereas the phosphorylation by Cdc28-cyclin B (35) has no effect on activity. These protein kinases also have differential regulatory effects on Pah1 location and on its susceptibility to degradation by the 20S proteasome. The cytosolic location of Pah1 is largely controlled by the Pho85-Pho80 phosphorylations of its seven target sites (33, 35, 37), and this regulation is accentuated by the phosphorylation of the unique PKA site Ser-10 (38). Data indicate that these phosphorylations cause the retention of Pah1 in the cytosol (33, 35, 37, 38). As discussed herein, the 7A mutations of the Pho85-Pho80 phosphorylation sites bypass the Nem1-Spo7-mediated dephosphorylations that are required for Pah1 membrane association and the PAP function to synthesize TAG (33, 35–37). The three Cdc28-cyclin B phosphorylation sites, which overlap with three of the Pho85-Pho80 sites (Fig. 1B), have a relatively small effect on Pah1 location and its physiological function (35, 37), and the PKC phosphorylation has no effect on the location and function to synthesize TAG (42). The CKII site mutation S705A caused an increase in membrane association, but unlike the 7A mutations, the S705A mutation did not bypass the requirement for the Nem1-Spo7 phosphatase (e.g. did not complement the temperature-sensitive phenotype or defect in TAG content of the *nem1Δ* mutant). This observation substantiates the importance of dephosphorylating the seven Pho85-Pho80 sites that also have a major stimulatory effect on PAP activity (43). None of the other CKII phosphorylation site mutations affected the localization of Pah1; nor did they have an appreciable effect on the complementation of the temperature sensitive phenotype caused by the *nem1Δ* mutation. With respect to Pah1 degradation, the phosphorylations by Pho85-Pho80 and PKA have the major role in protecting Pah1 from the 20S proteasome (37, 38, 44, 45), whereas the phosphorylation by PKC favors degradation, but only when the enzyme is not phosphorylated by Pho85-Pho80 (42). In contrast, the CKII phosphorylation had no effect on the degradation by the 20S proteasome.

The Nem1-Spo7 phosphatase plays a crucial role in governing the phosphorylation state of Pah1, and this protein phosphatase had the highest activity on the sites that are phosphorylated by Pho85-Pho80 (43), which is consistent with the major effects imparted by the 7A mutations (33, 35, 37). The activity of

Phosphorylation of Pah1 Phosphatidate Phosphatase by CKII

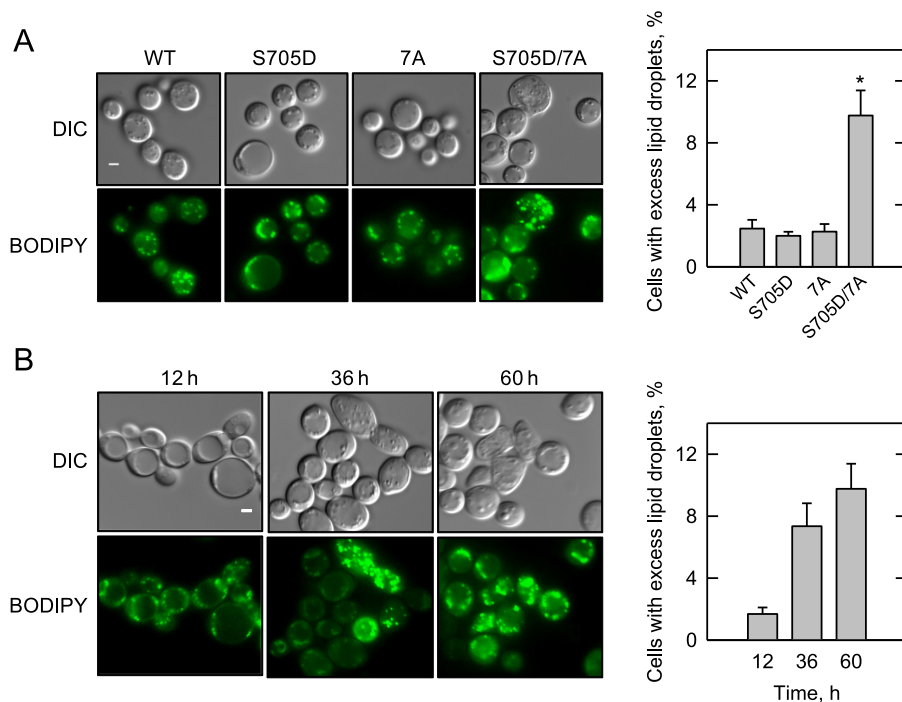


FIGURE 12. Lipid droplet synthesis is affected by the CKII phosphorylation state of Pah1 at Ser-705 in combination with its 7A mutations for the Pho85-Pho80 phosphorylation sites. *A*, the indicated wild type and phosphorylation site mutant forms of Pah1 were expressed in *pah1Δ* mutant cells and grown for 60 h (stationary phase). *B*, *pah1Δ* mutant cells expressing the Pah1 S705D/7A mutations were grown for the indicated time intervals. Lipid droplets were visualized by fluorescence microscopy after staining cells with BODIPY 493/503. The data shown are representative of several fields of view during multiple experiments. *Right panels*, the number of cells with an excess of lipid droplets (~20 droplets/cell) was counted in eight different frames having 300–800 cells/frame \pm S.D. (error bars). *DIC*, differential interference contrast. *White bar*, 1 μ m. *, $p < 0.05$ versus wild type.

the phosphatase toward the CKII phosphorylation sites was ~4-fold lower when compared with the Pho85-Pho80 sites but comparable with that of the sites phosphorylated by PKA. The Nem1-Spo7 phosphatase activity on the PKC sites was 14-fold lower than on the Pho85-Pho80 sites, which is consistent with the stimulatory effect PKC has on proteasomal degradation (42, 45); for proteasomal degradation, the Pho85-Pho80 sites should be dephosphorylated to allow for the phosphorylation by PKC.

The differential effects of the various protein kinases on Pah1 are further complicated by the hierarchical nature of the phosphorylations. For example, the prephosphorylation of Pah1 by Pho85-Pho80 inhibits its subsequent phosphorylation by PKC (42). As indicated above, this regulation impacts the susceptibility of Pah1 degradation by the 20S proteasome (42, 45). Here, we showed that the prephosphorylation of Pah1 by PKA or PKC reduces its subsequent phosphorylation by CKII and that its prephosphorylation by CKII reduces the subsequent phosphorylation by PKA. That CKII phosphorylation does not affect the phosphorylation by PKC suggests that the PKA site involved may be the unique site Ser-10 because three of the PKA and PKC sites overlap with each other (38, 42) (Fig. 1B). This in turn could have an impact on the effects of the Pho85-Pho80 phosphorylations of Pah1 as discussed above. However, at this point, we can only speculate on the importance of the hierarchical phosphorylations involving CKII because more work is needed to unravel this aspect of the multisite phosphorylations. Moreover, it is unclear when different protein kinases phosphorylate Pah1. We expect that Pah1 is primarily phosphorylated by Pho85-Pho80, Cdc28-cyclin B, and PKA in logarithmically

growing cells and by PKC as cells progress into quiescence because these are the stages of growth when these protein kinases exert their roles in cell physiology (94–96). The phosphorylation of Pah1 by CKII may occur at any growth stage, given that this protein kinase is constitutively active (55).

To explore the physiological effects of the CKII phosphorylation, the phosphorylation-deficient/mimicking mutants of Pah1 were examined for their ability to complement the temperature-sensitive phenotype caused by the *pah1Δ* and *pah1Δ nem1Δ* mutations and for their effects on TAG content. None of the mutants, alone or in combination, affected Pah1 function as assessed by these assays. However, this analysis revealed that the CKII phosphorylation-mimicking S705D mutation abrogates the Pho85-Pho80 phosphorylation-deficient 7A mutant complementation of the *pah1Δ* temperature-sensitive phenotype, but only when Nem1-Spo7 phosphatase is present. The lack of growth at 37 °C was not attributed to the mutations causing a temperature-sensitive PAP activity, indicating that the S705D/7A mutant enzyme is functional *in vivo* at 37 °C. Moreover, the S705D/7A mutant enzyme supported cell growth at the restrictive temperature when the Nem1-Spo7 phosphatase complex was absent. At the permissive temperature for growth, the S705D/7A mutations caused a significant increase (e.g. 70%) in TAG content, but again, only when the Nem1-Spo7 phosphatase complex was present. Moreover, the increase in TAG content correlated with a doubling of lipid droplet number per cell in about 10% of the mutant cell population.

That the Nem1-Spo7 phosphatase complex is required for the unique phenotypes caused by the S705D/7A mutations

raises the suggestion that dephosphorylation of sites other than the seven sites phosphorylated by Pho85-Pho80 must be important for Pah1 function at the membrane. The site(s) involved is unknown, but we do know that Nem1-Spo7 phosphatase utilizes Pah1 substrates that are phosphorylated by protein kinases other than Pho85-Pho80 (43) (Fig. 5). One explanation for the phenotypes imparted by the S705D/7A mutations is that the constitutive phosphorylation-mimicking S705D mutation, under the condition where the Pho85-Pho80 sites are already dephosphorylated (e.g. 7A mutations), might cause dephosphorylation of another site(s) to stimulate Pah1 function and increase TAG content. This condition, coupled to the increase in Pah1 activity at 40 °C (Fig. 10C), might be responsible for the lethal phenotype at the restrictive temperature (Fig. 10A, bottom). The basis for this lethality might be an excess of the PAP reaction product DAG that is known to be toxic to yeast growth (97). The toxic effect of elevated PAP function on cell growth (as mediated by the 7A mutations in combination with the PKA S10A mutation or the massive expression of the 7A mutations) has been observed previously (33, 35, 38). We understand that this scenario might be an oversimplification of the very complex regulation that occurs *in vivo*, but it does provide a plausible hypothesis for further study.

Pah1 in its major role in the synthesis of TAG (10, 17) has also been shown to be involved with lipid droplets (17, 19). In particular, the lack of Pah1 causes a reduction in lipid droplet number (17, 19). Screens of yeast mutants have identified several genes whose mutations also cause a reduction in lipid droplet number, and a population of those cells have lipid droplets with increased volume (e.g. so-called supersized lipid droplets) (98, 99). Interestingly, two of these genes, namely *CKB1* and *CKB2*, encode the regulatory subunits of CKII (99), implying that the CKII-mediated phosphorylation of some protein(s) is required for normal lipid droplet formation. The hypothesis that Pah1 is one of these proteins is supported by the observation that the combined S705D/7A mutations, which mimic the phosphorylation by CKII without phosphorylation by Pho85-Pho80, caused an increase in lipid droplet number.

CKII is essential to cell growth through phosphorylation of multiple proteins involved in gene expression, growth control, signal transduction, and cell cycle progression (52, 100, 101). With respect to lipid metabolism, CKII has been shown to phosphorylate and stimulate the function of the transcriptional repressor Opi1 (78). Opi1 (102), the negative regulatory component of the Ino2/Ino4/Opi1 regulatory circuit of lipid synthesis gene expression (26, 27, 103), is activated through its translocation from the nuclear/ER membrane into the nucleus, where it binds Ino2 of the Ino2-Ino4 activation complex to attenuate transcription of UAS_{INO}-containing phospholipid synthesis genes (26, 27, 103, 104). In its inactive state, Opi1 is tethered to the nuclear/ER membrane through its interactions with the membrane-associated protein Scs2 and PA (104). The dissociation of Opi1 from the membrane is controlled in part by the reduction in PA content (104), which is also regulated by Pah1 PAP activity (15, 33). Thus, CKII may exert its function in regulating lipid metabolism by orchestrating the coordinate phosphorylations of Opi1 and Pah1.

Author Contributions—L.-S. H. and W.-M. S. performed the experiments and prepared the manuscript. G.-S. H. and G. M. C. directed the research and contributed to the preparation of the manuscript. All authors analyzed the results and approved the final version of the manuscript.

Acknowledgments—We acknowledge Symeon Siniossoglou for supplying the *pah1Δ* and *pah1Δ nem1Δ* mutants used in this study. The mass spectrometry data were obtained from an instrument purchased in part by National Institutes of Health Grant NS046593 for the support of the Rutgers Mass Spectrometry Center for Integrative Neuroscience Research.

References

- Smith, S. W., Weiss, S. B., and Kennedy, E. P. (1957) The enzymatic dephosphorylation of phosphatidic acids. *J. Biol. Chem.* **228**, 915–922
- Pascual, F., and Carman, G. M. (2013) Phosphatidate phosphatase, a key regulator of lipid homeostasis. *Biochim. Biophys. Acta* **1831**, 514–522
- Carman, G. M., and Han, G.-S. (2009) Phosphatidic acid phosphatase, a key enzyme in the regulation of lipid synthesis. *J. Biol. Chem.* **284**, 2593–2597
- Brindley, D. N., Pilquill, C., Sariahmetoglu, M., and Reue, K. (2009) Phosphatidate degradation: phosphatidate phosphatases (lipins) and lipid phosphate phosphatases. *Biochim. Biophys. Acta* **1791**, 956–961
- Brindley, D. N., and Waggoner, D. W. (1996) Phosphatidate phosphorylase and signal transduction. *Chem. Phys. Lipids* **80**, 45–57
- Reue, K., and Brindley, D. N. (2008) Multiple roles for lipins/phosphatidate phosphatase enzymes in lipid metabolism. *J. Lipid Res.* **49**, 2493–2503
- Reue, K. (2009) The lipin family: mutations and metabolism. *Curr. Opin. Lipidol.* **20**, 165–170
- Reue, K., and Dwyer, J. R. (2009) Lipin proteins and metabolic homeostasis. *J. Lipid Res.* **50**, S109–S114
- Lin, Y.-P., and Carman, G. M. (1989) Purification and characterization of phosphatidate phosphatase from *Saccharomyces cerevisiae*. *J. Biol. Chem.* **264**, 8641–8645
- Han, G.-S., Wu, W.-I., and Carman, G. M. (2006) The *Saccharomyces cerevisiae* lipin homolog is a Mg²⁺-dependent phosphatidate phosphatase enzyme. *J. Biol. Chem.* **281**, 9210–9218
- Péterfy, M., Phan, J., Xu, P., and Reue, K. (2001) Lipodystrophy in the *fld* mouse results from mutation of a new gene encoding a nuclear protein, lipin. *Nat. Genet.* **27**, 121–124
- Donkor, J., Sariahmetoglu, M., Dewald, J., Brindley, D. N., and Reue, K. (2007) Three mammalian lipins act as phosphatidate phosphatases with distinct tissue expression patterns. *J. Biol. Chem.* **282**, 3450–3457
- Carman, G. M., and Han, G.-S. (2006) Roles of phosphatidate phosphatase enzymes in lipid metabolism. *Trends Biochem. Sci.* **31**, 694–699
- Csaki, L. S., Dwyer, J. R., Fong, L. G., Tontonoz, P., Young, S. G., and Reue, K. (2013) Lipins, lipinopathies, and the modulation of cellular lipid storage and signaling. *Prog. Lipid Res.* **52**, 305–316
- Santos-Rosa, H., Leung, J., Grimsey, N., Peak-Chew, S., and Siniossoglou, S. (2005) The yeast lipin Smp2 couples phospholipid biosynthesis to nuclear membrane growth. *EMBO J.* **24**, 1931–1941
- Han, G.-S., Siniossoglou, S., and Carman, G. M. (2007) The cellular functions of the yeast lipin homolog Pah1p are dependent on its phosphatidate phosphatase activity. *J. Biol. Chem.* **282**, 37026–37035
- Fakas, S., Qiu, Y., Dixon, J. L., Han, G.-S., Ruggles, K. V., Garbarino, J., Sturley, S. L., and Carman, G. M. (2011) Phosphatidate phosphatase activity plays a key role in protection against fatty acid-induced toxicity in yeast. *J. Biol. Chem.* **286**, 29074–29085
- Pascual, F., Soto-Cardalda, A., and Carman, G. M. (2013) PAH1-encoded phosphatidate phosphatase plays a role in the growth phase- and inositol-mediated regulation of lipid synthesis in *Saccharomyces cerevisiae*. *J. Biol. Chem.* **288**, 35781–35792
- Adeyo, O., Horn, P. J., Lee, S., Binns, D. D., Chandras, A., Chapman,

Phosphorylation of Pah1 Phosphatidate Phosphatase by CKII

- K. D., and Goodman, J. M. (2011) The yeast lipin orthologue Pah1p is important for biogenesis of lipid droplets. *J. Cell Biol.* **192**, 1043–1055
20. Sasser, T., Qiu, Q. S., Karunakaran, S., Padolina, M., Reyes, A., Flood, B., Smith, S., Gonzales, C., and Fratti, R. A. (2012) The yeast lipin 1 orthologue Pah1p regulates vacuole homeostasis and membrane fusion. *J. Biol. Chem.* **287**, 2221–2236
21. Lussier, M., White, A. M., Sheraton, J., di Paolo, T., Treadwell, J., Southard, S. B., Horenstein, C. I., Chen-Weiner, J., Ram, A. F., Kapteyn, J. C., Roemer, T. W., Vo, D. H., Bondoc, D. C., Hall, J., Zhong, W. W., et al. (1997) Large scale identification of genes involved in cell surface biosynthesis and architecture in *Saccharomyces cerevisiae*. *Genetics* **147**, 435–450
22. Ruiz, C., Cid, V. J., Lussier, M., Molina, M., and Nombela, C. (1999) A large-scale sonication assay for cell wall mutant analysis in yeast. *Yeast* **15**, 1001–1008
23. Siniosoglou, S. (2009) Lipins, lipids and nuclear envelope structure. *Traffic* **10**, 1181–1187
24. Siniosoglou, S. (2013) Phospholipid metabolism and nuclear function: roles of the lipin family of phosphatidic acid phosphatases. *Biochim. Biophys. Acta* **1831**, 575–581
25. Soto-Cardalda, A., Fakas, S., Pascual, F., Choi, H. S., and Carman, G. M. (2012) Phosphatidate phosphatase plays role in zinc-mediated regulation of phospholipid synthesis in yeast. *J. Biol. Chem.* **287**, 968–977
26. Carman, G. M., and Han, G.-S. (2011) Regulation of phospholipid synthesis in the yeast *Saccharomyces cerevisiae*. *Ann. Rev. Biochem.* **80**, 859–883
27. Henry, S. A., Kohlwein, S. D., and Carman, G. M. (2012) Metabolism and regulation of glycerolipids in the yeast *Saccharomyces cerevisiae*. *Genetics* **190**, 317–349
28. Koonin, E. V., and Tatusov, R. L. (1994) Computer analysis of bacterial haloacid dehalogenases defines a large superfamily of hydrolases with diverse specificity: application of an iterative approach to database search. *J. Mol. Biol.* **244**, 125–132
29. Madera, M., Vogel, C., Kummerfeld, S. K., Chothia, C., and Gough, J. (2004) The SUPERFAMILY database in 2004: additions and improvements. *Nucleic Acids Res.* **32**, D235–D239
30. Wu, W.-I., and Carman, G. M. (1996) Regulation of phosphatidate phosphatase activity from the yeast *Saccharomyces cerevisiae* by phospholipids. *Biochemistry* **35**, 3790–3796
31. Wu, W.-I., Lin, Y.-P., Wang, E., Merrill, A. H., Jr., and Carman, G. M. (1993) Regulation of phosphatidate phosphatase activity from the yeast *Saccharomyces cerevisiae* by sphingoid bases. *J. Biol. Chem.* **268**, 13830–13837
32. Wu, W.-I., and Carman, G. M. (1994) Regulation of phosphatidate phosphatase activity from the yeast *Saccharomyces cerevisiae* by nucleotides. *J. Biol. Chem.* **269**, 29495–29501
33. O'Hara, L., Han, G.-S., Peak-Chew, S., Grimsey, N., Carman, G. M., and Siniosoglou, S. (2006) Control of phospholipid synthesis by phosphorylation of the yeast lipin Pah1p/Smp2p Mg²⁺-dependent phosphatidate phosphatase. *J. Biol. Chem.* **281**, 34537–34548
34. Siniosoglou, S., Santos-Rosa, H., Rappsilber, J., Mann, M., and Hurt, E. (1998) A novel complex of membrane proteins required for formation of a spherical nucleus. *EMBO J.* **17**, 6449–6464
35. Choi, H.-S., Su, W.-M., Morgan, J. M., Han, G.-S., Xu, Z., Karanasios, E., Siniosoglou, S., and Carman, G. M. (2011) Phosphorylation of phosphatidate phosphatase regulates its membrane association and physiological functions in *Saccharomyces cerevisiae*: identification of Ser⁶⁰², Thr⁷²³, and Ser⁷⁴⁴ as the sites phosphorylated by CDC28 (CDK1)-encoded cyclin-dependent kinase. *J. Biol. Chem.* **286**, 1486–1498
36. Karanasios, E., Han, G.-S., Xu, Z., Carman, G. M., and Siniosoglou, S. (2010) A phosphorylation-regulated amphipathic helix controls the membrane translocation and function of the yeast phosphatidate phosphatase. *Proc. Natl. Acad. Sci. U.S.A.* **107**, 17539–17544
37. Choi, H.-S., Su, W.-M., Han, G.-S., Plote, D., Xu, Z., and Carman, G. M. (2012) Pho85p-Pho80p phosphorylation of yeast Pah1p phosphatidate phosphatase regulates its activity, location, abundance, and function in lipid metabolism. *J. Biol. Chem.* **287**, 11290–11301
38. Su, W.-M., Han, G.-S., Casciano, J., and Carman, G. M. (2012) Protein kinase A-mediated phosphorylation of Pah1p phosphatidate phosphatase functions in conjunction with the Pho85p-Pho80p and Cdc28p-cyclin B kinases to regulate lipid synthesis in yeast. *J. Biol. Chem.* **287**, 33364–33376
39. Karanasios, E., Barbosa, A. D., Sembongi, H., Mari, M., Han, G.-S., Reggiori, F., Carman, G. M., and Siniosoglou, S. (2013) Regulation of lipid droplet and membrane biogenesis by the acidic tail of the phosphatidate phosphatase Pah1p. *Mol. Biol. Cell* **24**, 2124–2133
40. Xu, Z., Su, W.-M., and Carman, G. M. (2012) Fluorescence spectroscopy measures yeast PAH1-encoded phosphatidate phosphatase interaction with liposome membranes. *J. Lipid Res.* **53**, 522–528
41. Barbosa, A. D., Sembongi, H., Su, W.-M., Abreu, S., Reggiori, F., Carman, G. M., and Siniosoglou, S. (2015) Lipid partitioning at the nuclear envelope controls membrane biogenesis. *Mol. Biol. Cell* **26**, 3641–3657
42. Su, W.-M., Han, G.-S., and Carman, G. M. (2014) Cross-talk phosphorylations by protein kinase C and Pho85p-Pho80p protein kinase regulate Pah1p phosphatidate phosphatase abundance in *Saccharomyces cerevisiae*. *J. Biol. Chem.* **289**, 18818–18830
43. Su, W.-M., Han, G.-S., and Carman, G. M. (2014) Yeast Nem1-Spo7 protein phosphatase activity on Pah1 phosphatidate phosphatase is specific for the Pho85-Pho80 protein kinase phosphorylation sites. *J. Biol. Chem.* **289**, 34699–34708
44. Pascual, F., Hsieh, L.-S., Soto-Cardalda, A., and Carman, G. M. (2014) Yeast Pah1p phosphatidate phosphatase is regulated by proteasome-mediated degradation. *J. Biol. Chem.* **289**, 9811–9822
45. Hsieh, L.-S., Su, W.-M., Han, G.-S., and Carman, G. M. (2015) Phosphorylation regulates the ubiquitin-independent degradation of yeast Pah1 phosphatidate phosphatase by the 20S proteasome. *J. Biol. Chem.* **290**, 11467–11478
46. Chi, A., Huttenhower, C., Geer, L. Y., Coon, J. J., Syka, J. E., Bai, D. L., Shabanowitz, J., Burke, D. J., Troyanskaya, O. G., and Hunt, D. F. (2007) Analysis of phosphorylation sites on proteins from *Saccharomyces cerevisiae* by electron transfer dissociation (ETD) mass spectrometry. *Proc. Natl. Acad. Sci. U.S.A.* **104**, 2193–2198
47. Li, X., Gerber, S. A., Rudner, A. D., Beausoleil, S. A., Haas, W., Villén, J., Elias, J. E., and Gygi, S. P. (2007) Large-scale phosphorylation analysis of α -factor-arrested *Saccharomyces cerevisiae*. *J. Proteome Res.* **6**, 1190–1197
48. Ubersax, J. A., Woodbury, E. L., Quang, P. N., Paraz, M., Blethrow, J. D., Shah, K., Shokat, K. M., and Morgan, D. O. (2003) Targets of the cyclin-dependent kinase Cdk1. *Nature* **425**, 859–864
49. Ptacek, J., Devgan, G., Michaud, G., Zhu, H., Zhu, X., Fasolo, J., Guo, H., Jona, G., Breitzkreutz, A., Sopko, R., McCartney, R. R., Schmidt, M. C., Rachidi, N., Lee, S. J., Mah, A. S., et al. (2005) Global analysis of protein phosphorylation in yeast. *Nature* **438**, 679–684
50. Dephoure, N., Howson, R. W., Blethrow, J. D., Shokat, K. M., and O'Shea, E. K. (2005) Combining chemical genetics and proteomics to identify protein kinase substrates. *Proc. Natl. Acad. Sci. U.S.A.* **102**, 17940–17945
51. Mah, A. S., Elia, A. E., Devgan, G., Ptacek, J., Schutkowski, M., Snyder, M., Yaffe, M. B., and Deshaies, R. J. (2005) Substrate specificity analysis of protein kinase complex Dbf2-Mob1 by peptide library and proteome array screening. *BMC Biochem.* **6**, 22
52. Glover, C. V., 3rd (1998) On the physiological role of casein kinase II in *Saccharomyces cerevisiae*. *Prog. Nucleic Acid Res. Mol. Biol.* **59**, 95–133
53. Litchfield, D. W. (2003) Protein kinase CK2: structure, regulation and role in cellular decisions of life and death. *Biochem. J.* **369**, 1–15
54. Guerra, B., and Issinger, O. G. (1999) Protein kinase CK2 and its role in cellular proliferation, development and pathology. *Electrophoresis* **20**, 391–408
55. Poole, A., Poore, T., Bandhakavi, S., McCann, R. O., Hanna, D. E., and Glover, C. V. (2005) A global view of CK2 function and regulation. *Mol. Cell Biochem.* **274**, 163–170
56. Chen-Wu, J. L., Padmanabha, R., and Glover, C. V. (1988) Isolation, sequencing, and disruption of the CKA1 gene encoding the α subunit of yeast casein kinase II. *Mol. Cell Biol.* **8**, 4981–4990
57. Reed, J. C., Bidwai, A. P., and Glover, C. V. C. (1994) Cloning and disruption of *CKB2*, the gene encoding for the 32-kDa regulatory β'

- subunit of *Saccharomyces cerevisiae* casein kinase II. *J. Biol. Chem.* **269**, 18192–18200
58. Bidwai, A. P., Reed, J. C., and Glover, C. V. (1995) Cloning and disruption of *CKBI*, the gene encoding the 38-kDa β subunit of *Saccharomyces cerevisiae* casein kinase II (CKII): deletion of CKII regulatory subunits elicits a salt-sensitive phenotype. *J. Biol. Chem.* **270**, 10395–10404
 59. Padmanabha, R., and Glover, C. V. C. (1987) Casein kinase II of yeast contains two distinct α polypeptides and an unusually large β subunit. *J. Biol. Chem.* **262**, 1829–1835
 60. Marin, O., Meggio, F., Marchiori, F., Borin, G., and Pinna, L. A. (1986) Site specificity of casein kinase-2 (TS) from rat liver cytosol. A study with model peptide substrates. *Eur. J. Biochem.* **160**, 239–244
 61. Bradford, M. M. (1976) A rapid and sensitive method for the quantitation of microgram quantities of protein utilizing the principle of protein-dye binding. *Anal. Biochem.* **72**, 248–254
 62. Han, G.-S., Sreenivas, A., Choi, M.-G., Chang, Y.-F., Martin, S. S., Baldwin, E. P., and Carman, G. M. (2005) Expression of human CTP synthetase in *Saccharomyces cerevisiae* reveals phosphorylation by protein kinase A. *J. Biol. Chem.* **280**, 38328–38336
 63. Rose, M. D., Winston, F., and Heiter, P. (1990) *Methods in Yeast Genetics: A Laboratory Course Manual*, Cold Spring Harbor Laboratory Press, Cold Spring Harbor, NY
 64. Sambrook, J., Fritsch, E. F., and Maniatis, T. (1989) *Molecular Cloning: A Laboratory Manual*, 2nd Ed., Cold Spring Harbor Laboratory, Cold Spring Harbor, NY
 65. Innis, M. A., and Gelfand, D. H. (1990) in *PCR Protocols: A Guide to Methods and Applications* (Innis, M. A., Gelfand, D. H., Sninsky, J. J., and White, T. J., eds) pp. 3–12, Academic Press, Inc., San Diego
 66. Ito, H., Fukuda, Y., Murata, K., and Kimura, A. (1983) Transformation of intact yeast cells treated with alkali cations. *J. Bacteriol.* **153**, 163–168
 67. Jeffery, D. A., Springer, M., King, D. S., and O'Shea, E. K. (2001) Multi-site phosphorylation of Pho4 by the cyclin-CDK Pho80-Pho85 is semi-processive with site preference. *J. Mol. Biol.* **306**, 997–1010
 68. Leggett, D. S., Glickman, M. H., and Finley, D. (2005) Purification of proteasomes, proteasome subcomplexes, and proteasome-associated proteins from budding yeast. *Methods Mol. Biol.* **301**, 57–70
 69. Laemmli, U. K. (1970) Cleavage of structural proteins during the assembly of the head of bacteriophage T4. *Nature* **227**, 680–685
 70. Boyle, W. J., van der Geer, P., and Hunter, T. (1991) Phosphopeptide mapping and phosphoamino acid analysis by two-dimensional separation on thin-layer cellulose plates. *Methods Enzymol.* **201**, 110–149
 71. Yang, W.-L., and Carman, G. M. (1995) Phosphorylation of CTP synthetase from *Saccharomyces cerevisiae* by protein kinase C. *J. Biol. Chem.* **270**, 14983–14988
 72. MacDonald, J. I. S., and Kent, C. (1994) Identification of phosphorylation sites in rat liver CTP:phosphocholine cytidyllyltransferase. *J. Biol. Chem.* **269**, 10529–10537
 73. Carman, G. M., and Lin, Y.-P. (1991) Phosphatidate phosphatase from yeast. *Methods Enzymol.* **197**, 548–553
 74. Guengerich, F. P., Wang, P., and Davidson, N. K. (1982) Estimation of isozymes of microsomal cytochrome P-450 in rats, rabbits, and humans using immunochemical staining coupled with sodium dodecyl sulfate-polyacrylamide gel electrophoresis. *Biochemistry* **21**, 1698–1706
 75. Burnette, W. (1981) Western blotting: electrophoretic transfer of proteins from sodium dodecyl sulfate-polyacrylamide gels to unmodified nitrocellulose and radiographic detection with antibody and radioiodinated protein A. *Anal. Biochem.* **112**, 195–203
 76. Haid, A., and Suissa, M. (1983) Immunochemical identification of membrane proteins after sodium dodecyl sulfate-polyacrylamide gel electrophoresis. *Methods Enzymol.* **96**, 192–205
 77. Choi, H.-S., Han, G.-S., and Carman, G. M. (2010) Phosphorylation of yeast phosphatidylserine synthase by protein kinase A: identification of Ser⁴⁶ and Ser⁴⁷ as major sites of phosphorylation. *J. Biol. Chem.* **285**, 11526–11536
 78. Chang, Y.-F., and Carman, G. M. (2006) Casein kinase II phosphorylation of the yeast phospholipid synthesis transcription factor Opi1p. *J. Biol. Chem.* **281**, 4754–4761
 79. Morlock, K. R., Lin, Y.-P., and Carman, G. M. (1988) Regulation of phosphatidate phosphatase activity by inositol in *Saccharomyces cerevisiae*. *J. Bacteriol.* **170**, 3561–3566
 80. Bligh, E. G., and Dyer, W. J. (1959) A rapid method of total lipid extraction and purification. *Can. J. Biochem. Physiol.* **37**, 911–917
 81. Henderson, R. J., and Tocher, D. R. (1992) in *Lipid Analysis* (Hamilton, R. J., and Hamilton, S., eds) pp. 65–111, IRL Press, New York
 82. Albuquerque, C. P., Smolka, M. B., Payne, S. H., Bafna, V., Eng, J., and Zhou, H. (2008) A multidimensional chromatography technology for in-depth phosphoproteome analysis. *Mol. Cell Proteomics* **7**, 1389–1396
 83. Holt, L. J., Tuch, B. B., Villén, J., Johnson, A. D., Gygi, S. P., and Morgan, D. O. (2009) Global analysis of Cdk1 substrate phosphorylation sites provides insights into evolution. *Science* **325**, 1682–1686
 84. Blom, N., Sicheritz-Pontén, T., Gupta, R., Gammeltoft, S., and Brunak, S. (2004) Prediction of post-translational glycosylation and phosphorylation of proteins from the amino acid sequence. *Proteomics* **4**, 1633–1649
 85. Huang, H. D., Lee, T. Y., Tzeng, S. W., and Horng, J. T. (2005) Kinase-Phos: a web tool for identifying protein kinase-specific phosphorylation sites. *Nucleic Acids Res.* **33**, W226–W229
 86. Swaney, D. L., Beltrao, P., Starita, L., Guo, A., Rush, J., Fields, S., Krogan, N. J., and Villén, J. (2013) Global analysis of phosphorylation and ubiquitylation cross-talk in protein degradation. *Nat. Methods* **10**, 676–682
 87. Smolka, M. B., Albuquerque, C. P., Chen, S. H., and Zhou, H. (2007) Proteome-wide identification of *in vivo* targets of DNA damage checkpoint kinases. *Proc. Natl. Acad. Sci. U.S.A.* **104**, 10364–10369
 88. Roach, P. J. (1991) Multisite and hierarchical protein phosphorylation. *J. Biol. Chem.* **266**, 14139–14142
 89. Irie, K., Takase, M., Araki, H., and Oshima, Y. (1993) A gene, SMP2, involved in plasmid maintenance and respiration in *Saccharomyces cerevisiae* encodes a highly charged protein. *Mol. Gen. Genet.* **236**, 283–288
 90. Chae, M., Han, G.-S., and Carman, G. M. (2012) The *Saccharomyces cerevisiae* actin patch protein App1p is a phosphatidate phosphatase enzyme. *J. Biol. Chem.* **287**, 40186–40196
 91. Chae, M., and Carman, G. M. (2013) Characterization of the yeast actin patch protein App1p phosphatidate phosphatase. *J. Biol. Chem.* **288**, 6427–6437
 92. Toke, D. A., Bennett, W. L., Dillon, D. A., Wu, W.-I., Chen, X., Ostrander, D. B., Oshiro, J., Cremesti, A., Voelker, D. R., Fischl, A. S., and Carman, G. M. (1998) Isolation and characterization of the *Saccharomyces cerevisiae* *DPP1* gene encoding for diacylglycerol pyrophosphate phosphatase. *J. Biol. Chem.* **273**, 3278–3284
 93. Toke, D. A., Bennett, W. L., Oshiro, J., Wu, W.-I., Voelker, D. R., and Carman, G. M. (1998) Isolation and characterization of the *Saccharomyces cerevisiae* *LPP1* gene encoding a Mg²⁺-independent phosphatidate phosphatase. *J. Biol. Chem.* **273**, 14331–14338
 94. Gray, J. V., Petsko, G. A., Johnston, G. C., Ringe, D., Singer, R. A., and Werner-Washburne, M. (2004) “Sleeping beauty”: quiescence in *Saccharomyces cerevisiae*. *Microbiol. Mol. Biol. Rev.* **68**, 187–206
 95. De Virgilio, C. (2012) The essence of yeast quiescence. *FEMS Microbiol. Rev.* **36**, 306–339
 96. Thevelein, J. M. (1994) Signal transduction in yeast. *Yeast* **10**, 1753–1790
 97. Fakas, S., Konstantinou, C., and Carman, G. M. (2011) *DGK1*-encoded diacylglycerol kinase activity is required for phospholipid synthesis during growth resumption from stationary phase in *Saccharomyces cerevisiae*. *J. Biol. Chem.* **286**, 1464–1474
 98. Fei, W., Shui, G., Gaeta, B., Du, X., Kuerschner, L., Li, P., Brown, A. J., Wenk, M. R., Parton, R. G., and Yang, H. (2008) Fld1p, a functional homologue of human seipin, regulates the size of lipid droplets in yeast. *J. Cell Biol.* **180**, 473–482
 99. Fei, W., Shui, G., Zhang, Y., Krahmer, N., Ferguson, C., Kapterian, T. S., Lin, R. C., Dawes, I. W., Brown, A. J., Li, P., Huang, X., Parton, R. G., Wenk, M. R., Walther, T. C., and Yang, H. (2011) A role for phosphatidic acid in the formation of “supersized” lipid droplets. *PLoS Genet.* **7**, e1002201
 100. Pinna, L. A. (2002) Protein kinase CK2: a challenge to canons. *J. Cell Sci.* **115**, 3873–3878
 101. Meggio, F., and Pinna, L. A. (2003) One-thousand-and-one substrates of protein kinase CK2? *FASEB J.* **17**, 349–368

Phosphorylation of Pah1 Phosphatidate Phosphatase by CKII

102. White, M. J., Hirsch, J. P., and Henry, S. A. (1991) The *OPI1* gene of *Saccharomyces cerevisiae*, a negative regulator of phospholipid biosynthesis, encodes a protein containing polyglutamine tracts and a leucine zipper. *J. Biol. Chem.* **266**, 863–872
103. Carman, G. M., and Henry, S. A. (2007) Phosphatidic acid plays a central role in the transcriptional regulation of glycerophospholipid synthesis in *Saccharomyces cerevisiae*. *J. Biol. Chem.* **282**, 37293–37297
104. Loewen, C. J. R., Gaspar, M. L., Jesch, S. A., Delon, C., Ktistakis, N. T., Henry, S. A., and Levine, T. P. (2004) Phospholipid metabolism regulated by a transcription factor sensing phosphatidic acid. *Science* **304**, 1644–1647
105. Kastaniotis, A. J., Autio, K. J., Sormunen, R. T., and Hiltunen, J. K. (2004) Htd2p/Yhr067p is a yeast 3-hydroxyacyl-ACP dehydratase essential for mitochondrial function and morphology. *Mol. Microbiol.* **53**, 1407–1421
106. Han, G.-S., O'Hara, L., Carman, G. M., and Siniosoglou, S. (2008) An unconventional diacylglycerol kinase that regulates phospholipid synthesis and nuclear membrane growth. *J. Biol. Chem.* **283**, 20433–20442
107. Thomas, B., and Rothstein, R. (1989) Elevated recombination rates in transcriptionally active DNA. *Cell* **56**, 619–630
108. Sikorski, R. S., and Hieter, P. (1989) A system of shuttle vectors and yeast host strains designed for efficient manipulation of DNA in *Saccharomyces cerevisiae*. *Genetics* **122**, 19–27